THE FIRST NINE MONTHS OF SN 1987A: WHAT HAVE WE LEARNT?

MICHAEL A. DOPITA

Mt. Stromlo and Siding Spring Observatories, The Australian National University, Canberra, ACT 2606, Australia

(Received 8 January, 1988)

Abstract. In the nine months since the explosion of SN 1987A, observations have been made throughout virtually the whole of the electromagnetic spectrum. This review attempts to summarize the observational results in the context of theoretical models, and presents what has been learnt about the physics of Type II supernova events from this extraordinary event.

1. Introduction

The death occurred suddenly, on February 23.316 UT of the rather ordinary-looking B-Supergiant star, Sk – 69°202 in the Large Magellanic Cloud. This event, which heralded the birth of the new discipline of extragalactic neutrino astronomy, was largely unexpected by both observers and theoreticians alike. In most of the literature prior to the event, blue supergiant stars had not been considered as candidates for Type II Supernova events. It is fortunate that the first naked-eye supernova in some 300 years did not conform to our comfortable preconceptions, since the learning process which ensued has been all the more intense.

In this *Review* I will attempt to demonstrate that since the event, we have achieved a good level of understanding of the peculiar photometric and dynamic properties of this supernova, in particular, the reasons for the exceptional dimness of this event, the very slow and steady rise to maximum light, and the very rapid initial evolution of the fireball. The effects of the supernova on the development of scientific thought are only just now becoming clear. These are far ranging, and cover stellar evolution, mass loss and mixing, the physics of core collapse, particle physics, the chemical evolution of galaxies, the physics of the interstellar medium and X- and γ-ray astronomy to name but a few.

I dedicate this *Review* to the memory of Iosiph Samuilovitch Shklovski (1916–1985). Regrettably, the LMC is just two light years too far away, and he never saw the event. However, this visionary man had achieved a clear appreciation of two key facts required for the understanding of SN 1987A. He realized that adiabatic losses in the shocked outer layers would ensure that compact pre-supernova stars would produce only dim optical events. He also pointed out that the apparent lack of SN II in irregular galaxies is probably due to observational selection against the detection of dim supernova events (such as SN 1987A), and is probably due to the difficulty of forming an extended envelope at low metallicity (Shklovski, 1984, 1985).

Space Science Reviews **46** (1988) 225–271.

2. The Nature and Evolution of the Precursor

There is now no doubt that SN 1987A is positionally coincident with the B3I star, Sk – 69°202. This has been established by astrometry with a positional accuracy of 0.1 arc sec, or less (White and Malin, 1987a, b; West *et al.*, 1987; see Figure 2.1). This

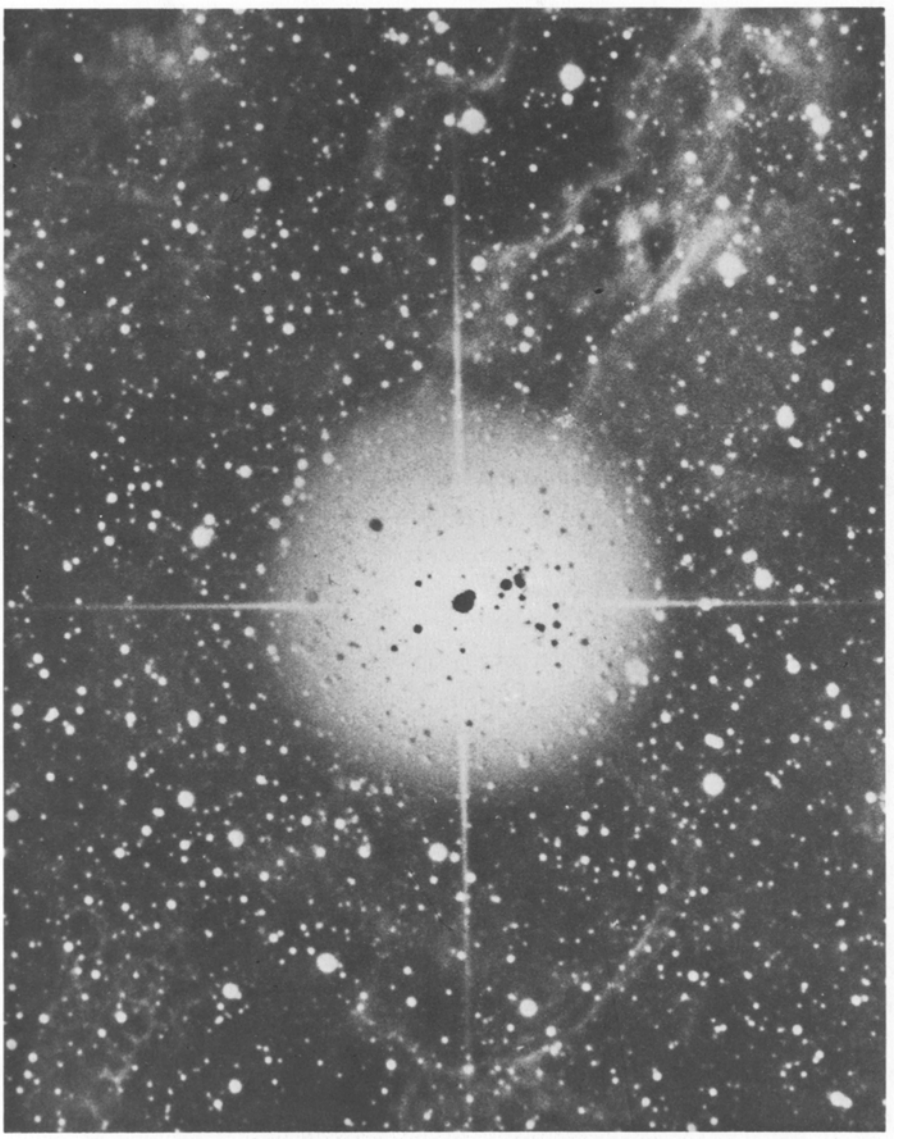

Fig. 2.1. A photographic superposition of a pre-supernova UK Schmidt Telescope plate (negative), and a post-supernova plate (positive), prepared by David Malin of the Anglo-Australian Telescope. The alignment of the diffraction spikes shows clearly that the star which exploded was the brighter of the components of the image of Sk – 69°202.

star was characterized by the following photometric parameters (Rousseau *et al.*, 1978):

$$V = 12.24\,, \qquad (B - V) = 0.04\,, \qquad (U - B) = -0.65\,.$$

The identification of Sk – 69°202 with the supernova event was initially confused by the fact that the star has two close companions and appears as a composite image in most extant photographs (West *et al.*, 1987; Shara *et al.*, 1987; Walborn *et al.*, 1987, see Figure 2.1). The brighter of these, dubbed star # 2, is some 3 arc sec away at Pa 315°, and has $V = 15.3$, $(B - V) = 0.2 \pm 0.4$. The fainter companion, star # 3, is about 1.5 arc sec away, at PA 120°, and has $(B - V) = 0.15 \pm 0.4$. When the supernova faded very rapidly in the UV, the detection of UV emission from star # 3 was first interpreted as showing that Sk – 69°202 had not in fact exploded (Cassatella *et al.*, 1987a; Sonneborn and Kirshner, 1987). In late March the situation was still confused but the possibility of the UV signal being a result of star # 3 had been mooted (Panagia *et al.*, 1987). Recently, two independent analyses of the UV data have revealed beyond any shadow of a doubt that Sk – 69°202 has in fact exploded (Gilmozzi *et al.*, 1987; Sonneborn *et al.*, 1987).

The reddening to this star remains somewhat uncertain, and this is the main source of error in our determination of the bolometric luminosity of the event. From a measurement of the Balmer decrement of the surrounding H II region, Danziger *et al.* (1987) find $A_v = 0.66 \pm 0.2$. This seems to be somewhat high by comparison with other determinations, and may be a result of some collisional excitation of the Balmer lines. Wampler *et al.* (1987) use the observed absolute strength of the λ5780 Å and λ5797 Å diffuse interstellar bands (Vladilo *et al.*, 1987) to estimate $A_v = 0.45$. These estimates should both be somewhat reduced to take account of the fact that the ratio of total to selective extinction is rather lower in the LMC than in the Galaxy, about 2.9 (e.g., Fitzpatrick, 1985). The diffuse interstellar band at λ6613 Å shows the LMC feature to be only about 75% as strong as the galactic component (Vidal-Majar *et al.*, 1987). The contribution of the galactic dust to the LMC line-of-sight reddening has been rather accurately measured at $E(B - V) = 0.034$ (McNamara and Feltz, 1980). This applies to the Shapley Constellation III region, and is somewhat lower than the value of 0.06 obtained including the stars in the 30 Dor region (Brunet, 1975; Isserstedt, 1975). However, it is harder to measure the galactic contribution accurately in such a region of higher local reddening, especially in view of the different galactic and LMC reddening laws. These values lead to an estimate of A_v in the range 0.18 up to 0.32. On the basis of this discussion, we adopt a value of $A_v = 0.3$, $E(B - V) = 0.11$.

Wood and Faulkner have stimated the following physical parameters:

$$M_{\rm bol} = -7.71\,, \qquad \log(L/L_\odot) = 4.98\,, \qquad \log T_{\rm eff} = 4.11\,.$$

These figures define Sk – 69°202 to be an entirely unremarkable blue supergiant star with a helium core mass of about $6\,M_\odot$ (see Figure 2.2).

Conventional wisdom had it that Supernovae of Type II occur either in red supergiants, or perhaps, in the Wolf–Rayet phase of evolution. The central problem for the evolutionary models is, therefore, how can the moment of core collapse be contrived

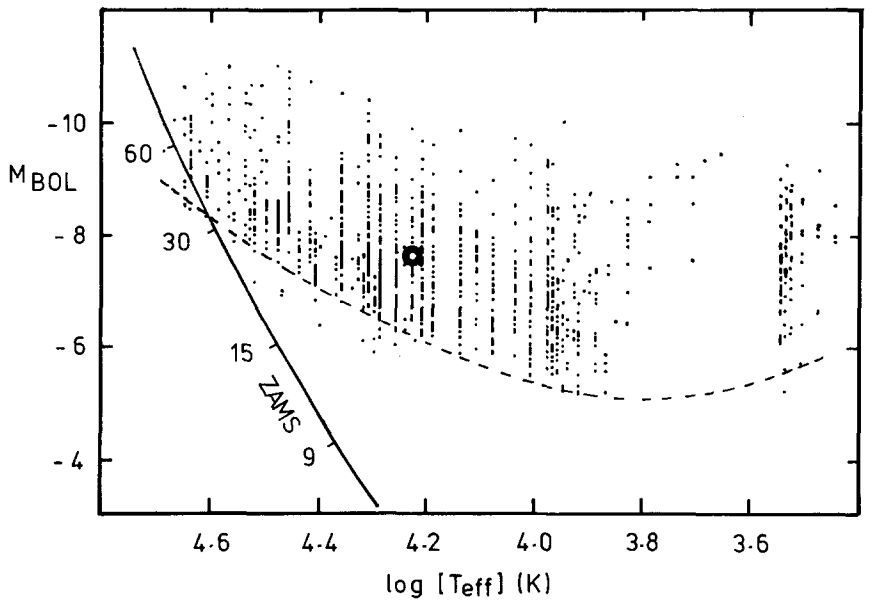

Fig. 2.2. The position of Sk – 69°202 in the HR-diagram (bold symbol) superimposed on the distribution of supergiant stars in the LMC according to Humphreys and McElroy (1984). The dotted line indicates the approximate survey limit, and the zero-age Main Sequence is also shown. Note in particular the existence of red supergiant stars at greater luminosity than Sk – 69°202.

to occur in a blue supergiant star? There have already been many attempts made to address this question, and from these it is apparent that the main sequence mass must have been in the range 15–20 $M_{\odot}$, though with some uncertainty determined by the relation between core and Main-Sequence mass, which is in turn a function of the convective overshooting during the hydrogen burning phase of evolution.

The theoretical models teach us that the end-point of evolution is remarkably sensitive to the assumptions and approximations made, and that the subject of the advanced stages of evolution of massive stars is by no means a closed book. The major parameters which determine the outcome are, in no particular order, the opacity, the treatment of convection and the treatment of mass loss.

In general, the decrease in opacity obtained with the lower abundances characteristic of the LMC tends to help to confine the evolutionary tracks to the blue side of the H–R diagram. However, most models are computed with the abundance set taken as solar divided by, say, four. In practice, the LMC abundance distribution is not this simple. Dopita (1986) and Russell *et al.* (1987) have shown that, in the LMC, the underabundance of various elements with respect to solar is strongly dependent upon their atomic number. For example, C and N are depleted by about 0.8 dex, O and Ne by about 0.5 dex, Ca by some 0.3 dex, and the heavy elements from Ti through Fe to Ba by 0.2 dex. This pattern is similar to that produced in models of deflagration supernovae, and may indicate that stars of a somewhat lower mass have been relatively more important in enriching the interstellar medium in the LMC than is the case for the Galaxy.

An important constraint in the evolutionary models is that they should correctly describe the observed ratio of red to blue supergiants in the LMC (Wood and Faulkner 1987; Maeder *et al.*, 1987). In the case of SN 1987A, the precursor star must have evolved first to the red and then back towards the blue, since red supergiants are observed at a higher luminosity than the precursor (see Figure 2.2), and the luminosity is a measure of the helium core mass, which has to increase monotonically. Many models without mass loss fail to do this, and never evolve to the red supergiant phase at all (Arnett, 1987a; Hillebrandt *et al.*, 1987c). However, this problem is code dependent for reasons that are not yet clear, and others do indeed evolve to the red before returning (Woosley *et al.*, 1987; Woosley, 1987; see Figure 2.3).

Models involving mass loss are more successful in reproducing the observed ratio of blue to red supergiants. Those which include convective overshooting (Maeder, 1987) have a somewhat higher core mass, and a larger residual hydrogen envelope than those which do not. Maeder argues that a result of mass loss is the dissapearance of the intermediate convective shell, which drives the expansion of the star to the red, even with low metallicity. The Wood and Faulkner (1987) model for a 17.5 $M_{\odot}$ precursor star is in many respects a fully self-consistent model. It contains the correct opacity for the observed LMC abundances, and uses Waldron (1985) mass-loss rates which correctly reproduce the blue to red supergiant ratio. The supernova occurs in these models when

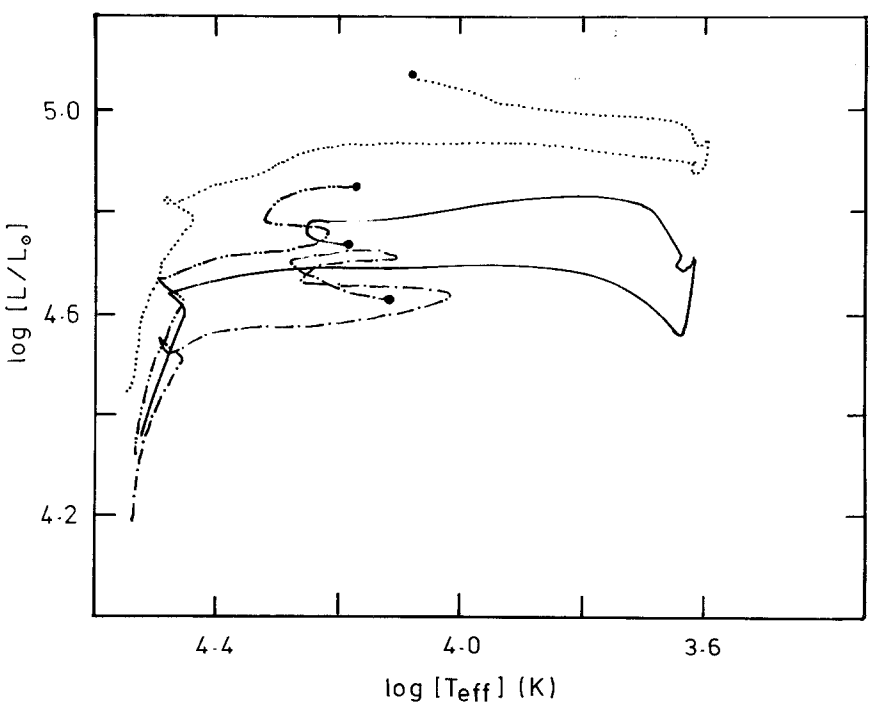

Fig. 2.3. A selection of some of the theoretical tracks to describe the pre-supernova evolution of Sk – 69°202. These are respectively; solid line, Woosley *et al.* (1987); dotted line, Wood and Faulkner (1987); dash-dotted line, Arnett (1987a); dash-double-dotted line, Hillebrandt *et al.* (1987c). Models for single-star precursor which fail to evolve to the red are excluded on observational grounds.

the helium core mass is 5.2 $M_\odot$ and only 0.2–0.6 $M_\odot$ of hydrogen is left on the star. Hydrogen shell burning has been extinguished before the supernova explosion. Theoretical estimates of the residual mass of the hydrogen envelope at the time of the explosion thus range from about 0.3 $M_\odot$ all the way up to about 10 $M_\odot$. Some observational data tends to support the lower values. The strength of the nitrogen lines in the precursor (Walborn, 1987), and the appearance of narrow N V, N IV], and N III] lines in the UV some weeks after the explosion (Kirshner, 1987) all suggest that CN processed material was not only abundant in the surface layers, but indeed, had been ejected in a previous red-giant phase. The appearance of X-ray emission at early epochs and the early appearance of lines of *s*-process elements in the spectra (Williams, 1987) (He-burnt material at the photosphere) also gives observational support for lower values of the total mass of the pre-supernova star unless substantial post-SN mixing has occurred. However, the energetics of the explosion (Woosley, 1987; Wheeler *et al.*, 1987a; and Nomoto *et al.*, 1987) would suggest high residual hydrogen mass, since in the low-mass scenario the hydrogen layers would be ejected at velocities much higher than those observed for any reasonable explosion energy. Also, the rise ot the maximum would have occurred on much too short a time-scale (Wheeler *et al.*, 1987b).

Barkat and Wheeler (1988) have made a careful study of the range of possible pre-supernova envelope structures. For fixed luminosity, helium core mass, and envelope composition, the self-consistent envelope solutions which match both the core properties and the observed surface temperature fall into two families. With normal hydrogen abundance, only models with very small residual hydrogen envelopes ($\sim 0.1\, M_\odot$) or, alternatively, large envelope mass can exist. The range of excluded envelope mass decreases as the helium content is increased until for $Y \geq 0.5$, no envelope solutions can be excluded on purely structural grounds.

3. The Core Collapse

Neutrino bursts have long been expected to be the first sign of a nearby supernova outburst, since they are the result of photodisintegration and collapse of the iron core. The optical outburst, on the other hand, is delayed at least until the moment of shock breakout through the photosphere.

The detection of the neutrinos from SN 1987A heralded the birth of extragalactic neutrino astronomy. In the literature, two separated neutrino events were reported from three separate facilities. The first of these was reported by the Mont Blanc Neutrino Observatory at February 23.120 UT (Aglietta *et al.*, 1987), whereas the second, occurring on February 23.316, was detected at both the Kamiokande-II collaboration in Japan and IMB neutrino experiment in the United States (Hirata *et al.*, 1987; Bionta *et al.*, 1987). The failure of the Kamiokande experiment to detect the Mont Blanc event (Krauss, 1987; Suzuki and Sato, 1987), and the oppressive energy requirements implied by the Mt. Blanc observations (Shaeffer *et al.*, 1987c) strongly suggests that the Mt. Blanc result may be spurious. This conclusion tends to be supported by arguments based on the time delay between the neutrino event and the appearance of optical

emission (Arnett, 1987; Shigeyama *et al.*, 1987; Wampler *et al.*, 1987). Hillebrandt *et al.* (1987a) and Haubold *et al.* (1987) have developed a scenario in which the first event is associated with core collapse to a neutron star, whereas the second is associated with a subsequent collapse of the neutron star to a black hole. However, in this case, it is hard to see how the first event would give a signal which looked more like that associated with the formation of a black hole, whilst the second is consistent with the formation of a neutron star in the standard scenario (e.g., Brown *et al.*, 1981).

The initial hope was that the dispersion in time of a neutrino burst could be used to estimate a neutrino rest mass (Bahcall 1987a, b) because the velocity of propagation of a neutrino depends on both its rest mass and its energy. From an analysis of the 13 events seen by the Kamiokande-II experiment, Hillebrandt *et al.* (1987b) see evidence for two neutrino species, with rest masses of about 8 and 20 eV c^{-2}, respectively. If, however, the duration of the neutrino burst is set by the diffusion time for trapped neutrinos to escape from the core of the neutron star (Arnett, 1987b), then clearly we cannot put any useful limits on the neutrino mass.

The expected sequence of events leading to a neutrino burst is as follows (Brown *et al.*, 1981; Bethe *et al.*, 1982). First, the iron core of the massive star is pushed over the edge of stability by the exhaustion of energy sources and by the onset of photodisintegration processes. During the collapse, most of the protons are transformed into neutrons, with the emission of $\bar{\nu}_e$ with energies less than about 10 MeV. The escape of these is inhibited after a few milliseconds when the infalling matter becomes opaque to neutrinos. When the collapsed core reaches nuclear densities, a shock is reflected outwards, and produces a second short low-energy burst of $\bar{\nu}_e$ when it passes into the lower density material still accreting to the core about 100–300 ms after the onset of the collapse. The remainder of the gravitational energy is radiated away in the form of $\nu\,\bar{\nu}$ pairs of all flavours (e, μ, τ). Only the lowest energy neutrinos are emitted, because their mean free path in nuclear matter is very energy dependent. Thus, the diffusion process takes several seconds to complete.

Analysis of the IMB and Kamiokande-II observations (Krauss, 1987; Sato and Suzuki, 1987; Suzuki and Sato, 1987) shows good agreement with the theoretical expectations. Suzuki and Sato (1987) assume that the neutrino spectrum could be fitted by a Fermi–Dirac distribution with temperature T and the chemical potential μ. The major source of events in a water Cherenkov detector is the $\bar{\nu}_e p \rightarrow e^+ n$ reaction with cross section $\sigma(E)$. The scattering cross-section for the $\bar{\nu}_e - e^-$ process is about 1.4% of this, and the $\bar{\nu}_e - O^{16}$ scattering cross-section is also only a few percent of the $\bar{\nu}_e - p$ reaction (Krauss, 1987). The expected number of events in the time interval Δt is then:

$$N(T, \mu, R, \Delta t) = N_{\text{tar}} \int F(E, T, \mu, R)\sigma(E)\varepsilon(E)\,\mathrm{d}E\,\Delta t\,, \tag{3.1}$$

where N_{tar} is the number of hydrogen atoms in the detector (2140 tons at Kamiokande; 5000 tons at IMB), $\varepsilon(E)$ is the efficiency function of the detector, and $F(E, T, \mu, R)$ is the neutrino flux at Earth from a neutrinosphere of radius R at a distance d:

$$F(E, T, \mu, R) = [\pi R^2/h^3 c^3 d^2]\,\frac{E^2}{\{1 + \exp[(R - \mu)/T]\}}\,. \tag{3.2}$$

The results of the analyses (Bahcall *et al.*, 1987a, b; Bruenn, 1987; Burrows and Lattimer, 1987; Krauss, 1987; Fukugita and Nakamura, 1987) are in general agreement with the theoretical expectation for the neutrino luminosity and neutrino temperature from a supernova which forms a $1.4\,M_{\odot}$ neutron star ($1\text{–}4 \times 10^{53}$ ergs; Brown *et al.*, 1981; Bethe *et al.*, 1982; Burrows, 1984; Wilson *et al.*, 1986). These results confirm the expectation that the dominant supernova neutrino cooling results from thermalized neutrino pairs diffusing from the edge of the neutrinosphere.

A detailed analysis of the time dependence of the neutrino signal may indicate the presence of some interesting physical effects. Harwit *et al.* (1987) find marginal evidence that the neutrino signal is pulse-modulated with a period of 8.9 ms, which could be related with the rotation period of a very young pulsar. Suzuki and Sato (1987) find that the data for the first second can be fitted with equations of the form of (3.1) and (3.2) provided that $T \sim 2$ MeV. If $\mu = 4T$, $R \sim 100$ km, and if $\mu = 0$ then $R \sim 30$ km. The signal in this period can be identified with the strong burst expected when the iron core becomes neutronized during the initial collapse and shock reflection phases. During the following 4 s, the Kamiokande data give $T \sim 5$ MeV and $\mu = 0$ with $R \sim 10$ km. This result can be understood if the proto-neutron star is born with a larger radius (cf. Wilson *et al.*, 1986; Hillebrandt, 1985) and has a neutrinosphere for which the diffusion of neutrinos is strongly energy dependent. It contracts to its final value of about 10 km in a few seconds. This contraction increases the temperature by adiabatic compression. However, during this time, the density at the surface becomes much higher and the radius of the neutrinosphere is then no longer dependent on energy.

The last three events observed at the Kamiokande-II facility are difficult to account for on standard models. Although they have a low characteristic energy, which could be accounted for by cooling, their late arrival times (5–13 s) nevertheless imply a large total energy for the event; in the region of $5\text{–}7 \times 10^{52}$ ergs. They probably are not the tail of the preceding burst, but may be produced by late-time non-spherical mass accretion due to the magnetic field and rotation Fukugita and Nakamura, 1987). An alternative hypothesis is that they are released in the phase transition in the core, which would release energy and allow further contraction of the core.

4. Shock Breakout

The light curves resulting from the explosion of a compact precursor were perhaps first calculated by Imshennik and Nadyozhin (1964). These show that the 'plateau' luminosity is reached very quickly, and that adiabatic losses in the expansion cause a dim optical display. The optical outburst clearly cannot occur until the shock wave resulting from the core collapse and bounce reaches the surface, and the surface has cooled to the point where it starts to emit in the optical. The early observations show that this had not occurred by February 23.39 UT (Jones; reported in Wampler *et al.*, 1987), but by February 23.44 UT the supernova was seen to have reached mag 6 (McNaught, 1987). There is also a colour photograph of the supernova taken on February 23.54 UT in New Zealand which shows the supernova as a blue object of

mag 5–6 (Ryder, 1987, private communication). The time of propagation of the shock to the surface, t_{prop}, is, therefore, less than 184 min and greater than 106 min, on the basis of the Kamiokande-II timing. This puts very stringent limits on the size of the precursor star (Grassberg *et al.*, 1987; Woosley, 1987; Wampler *et al.*, 1987; Shigeyama *et al.*, 1987). From a hydrodynamic model of the shock propagation, based on an instantaneous deposition of energy at the boundary of the neutronized core Shigeyama *et al.* (1987) derive:

$$t_{\text{prop}} = 19[R_0/10^{12}\text{ cm}]\,[M_{ej}/M_\odot]^{1/2}\,[E_0/10^{51}\text{ erg}]^{-1/2}\text{ min}\,. \tag{4.1}$$

M_{ej}, the ejected mass, probably lies in the range 7–12 $M_\odot$, the explosion energy, E_0, would have to lie in the range (0.5–1.5) $\times$ 10^{51} ergs (see below). The difference between this figure and the energy lost by the neutrino emission (1–4) $\times$ 10^{53} ergs, exemplifies the central problem in producing supernova explosions, namely the very low energetic efficiency with which the collapse is coupled with the explosion. Indeed, it is not at all clear that the major source of energy input to the ejecta is core-bounce followed by a prompt explosion (e.g., Hillebrandt, 1985). In most stellar models the final explosion energy is generated by explosive burning in the oxygen shell, and is, therefore, determined by the properties of those portions of the star which lie outside the core (Wilson *et al.*, 1986).

These initial parameters, when substituted in Equation (4.1) confine the initial radius, R_0, to lie in the range $1.1 \times 10^{12} < R_0 < 4.2 \times 10^{12}$ cm; allowing for the fact that the atmosphere must cool by adiabatic expansion before an optical display is seen. This is in good agreement with the identification of the precursor as a B3I star.

The initial luminosity of the supernova is entirely determined by energy deposited by the shock which is either advected to the photosphere, or which escapes by diffusion from the interior. The first term is much less important and amounts to $4v_{\text{exp}}/c$ times the diffusion luminosity. The initial luminosity and colour evolution is well represented by models which choose the correct combination of radius and energy deposited/unit mass (Grassberg *et al.*, 1987; Shigeyama *et al.*, 1987; Arnett, 1987a), since the luminosity, $L \propto \kappa^{-1} R_0[E_{th}/M]$, where κ is the opacity, and E_{th}/M is the thermal energy content per unit mass (Falk and Arnett, 1977; Arnett, 1980). Note that in the early diffusive release of energy, E_{th}/M may not necessarily be the same as E_0/M_{ej}, since the first is determined by the conditions of shock propagation throughout the outer layers, whereas the second is a global parameter. In fact, because of adiabatic losses, the time variation of E_{th}/M is $E_{th}/M \propto t^{-2}$ for a homologous expansion. However, because of the strong acceleration of the shock in the outer layers, the early expansion is not homologous, and the observed variation in the Bolometric luminosity was $L \propto t^{-0.7}$.

A prompt radio burst was related to the epoch of shock break-out. The burst reached a maximum in only a few days before fading in a similar time-scale (see Figure 4.1; Turtle *et al.*, 1987). The rise time was very much shorter, and the peak luminosity very much less than well-observed Type II supernovae such as SN 1979C or SN 1980K (Weiler, 1985). However, the physical process of the radio emission process in both SN 1987A and these much brighter radio supernova appears to be the same, namely,

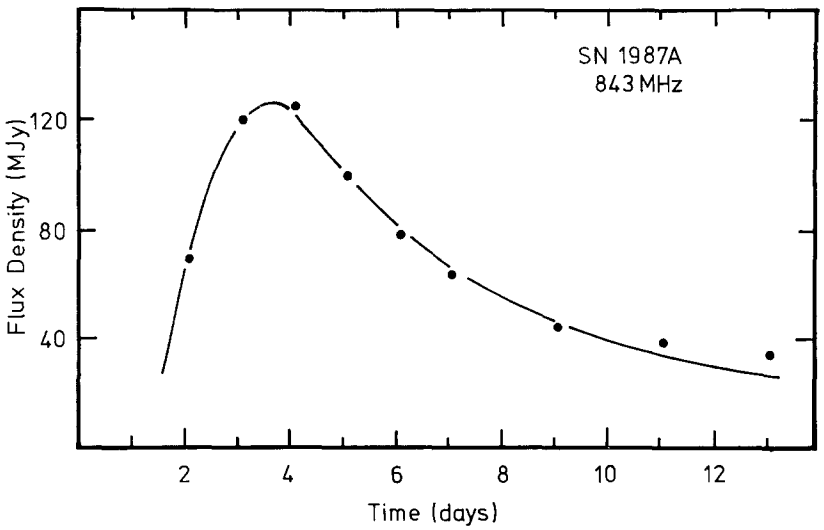

Fig. 4.1. The radio burst of SN 1987A as observed at 843 MHz at Molongolo Radio Observatory in Australia (Turtle *et al.*, 1987). The solid curve shows the best-fit model of Storey and Manchester (1987) which has internal free-free and synchrotron self-absorption included. An only slightly worse fit is obtained in a model in which the absorption arises in an ionized wind (Chevalier and Fransson, 1987).

free-free absorbed synchrotron emission (Storey and Manchester, 1987). The location of this radio emission was probably in the shocked stellar wind region of the star, with the free-free absorption arising either from within this layer, or from the unshocked but ionized region above it. Chevalier and Fransson (1987) and Dopita *et al.* (1987c) both find that the free-free absorption is consistent with it arising in the pre-supernova stellar wind. The parameters of this wind are estimated by both authors to lie in the range $(6\text{–}9) \times 10^{-5} M_{\odot}\ \mathrm{yr}^{-1}$ at a velocity of about 550 km s^{-1}. This is consistent with what was known about the luminosity and colour precursor star and, therefore, what its likely mass-loss would be using the Waldron (1984) figures (Dopita *et al.*, 1987c). The thickness of the emitting layer was estimated by Storey and Manchester (1987) to be only about 4.8% of the radius, which would be consistent with a power law density distribution of matter in the post-shock material with an index of 11.8. Since the first week, the radio emission has continued to fade (despite some other reports to the contrary), becoming effectively unobservable at 843 MHz after about 50 days. VLBI observations were conducted within a few days of the explosion. The radio disk was not observed, and this implies a velocity of expansion of more than 15 000 km s^{-1}. The time of transition from optically thick to optically thin radio emission (about 4 days) would suggest a blast-wave velocity as high as 30 000 km s^{-1}, which can be compared with the greatest absorption velocities seen in Hα at early times, which was also close to 30 000 km s^{-1}.

The epoch of shock breakout from the photosphere resulted in a 'flash' of UV photons, although probably not a very intense one (Chevalier and Fransson, 1987;

Dopita *et al.*, 1987c). From the early photometric data we find that the photospheric temperature (T_{eff}) can be fitted by the regression relation:

$$\log(T_{\text{eff}}) = (7.47 \pm 0.23) - (0.64 \pm 0.04) \log(t) .$$

Shock breakout probably occurred at about $\log(t) = 3.6$, and at this time the above regression gives a photospheric temperature, $T_{\text{eff}} \sim 150\,000$ K. This should be compared with the estimate derived on the assumption that, at the time of shock breakout, the shock is driven by radiation pressure, which gives $T_{\text{eff}} \sim 230\,000$ K. The effective temperature fell below the point where appreciable numbers of ionizing photons would be emitted in only 8–12 hr. The UV flash can, therefore, be characterized by a temperature of order $1–2 \times 10^5$ K, a luminosity of $2 \times 10^8 L_\odot$ and a duration of 2–4 hr. These parameters are consistent with the absence of any detectable effect on the Earth's ionosphere (Edwards, 1987). Dopita *et al.* (1987c) and Chevalier and Fransson (1987) proposed that this flash would be effective in ionizing the precursor stellar wind. Fluorescent ionization of a dense blob of gas lost to the star in the red giant phase may give an explanation of the 'mystery spot' discovered by speckle interferometry (Karovska *et al.*, 1987, Marcher *et al.*, 1987). This point is developed in Section 8.

During the initial phase of evolution ($t < 5$ days), the photosphere of the fireball grew almost linearly with time. The velocity of expansion inferred during this phase is 7700 km s^{-1}. This velocity is very similar to the value of 8000 km s^{-1} inferred from the hydrogen line profile in this epoch (Chugaj, 1987). At this time, the photosphere can be regarded as being trapped in the very steep outer density gradient produced by the shock as it broke through the pre-supernova photosphere and accelerated off into the wind region.

5. The Light and Colour Evolution

In Figures (5.1) and (5.2), we show the V magnitudes and the colour evolution for the first 250 days. In these figures are plotted all the published ground-based photometry. The compact initial state of the supernova ensured a rapid decrease in temperature through adiabatic losses. Thus, the initial colour evolution was about five times faster than what is normally observed in Type II supernovae. At about four days the $(B - V)$ and, more particularly, the $(U - B)$ colour evolution accelerated as line blanketing, initially from higher members of the Balmer series, but later from metal lines, mainly from the iron group, became important.

The climb towards maximum was accomplished at an almost constant temperature as measured by the $(V - I)$ colour, but a further decline in temperature was seen in the post-maximum phase as the luminosity collapsed towards the radioactive tail. An increase in $(U - B)$ occurred at 40–50 days, but this does not correspond to any change in photospheric temperature, and is presumably the result of a composition change working its way out to the photosphere.

After 125 days the V light curve followed the exponential decline expected if it was being powered by radioactive processes. Spectroscopic data taken in this period show

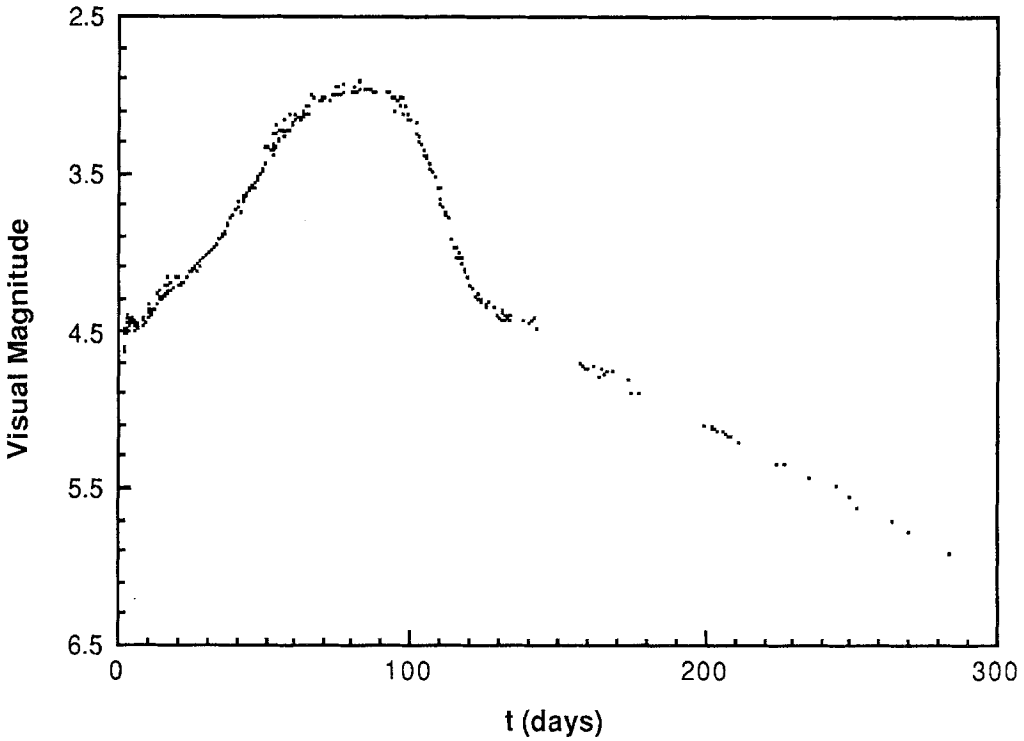

Fig. 5.1. The visual light curve for the first 300 days of SN 1987A. This shows the relatively slow and steady climb up to the plateau-like maximum, followed by the relatively rapid decine to the extended radioactively-powered exponential tail.

that the UV line blanketing is decreasing once again, which probably accounts for the decrease in $(U - B)$. However, the most important spectral development is the onset of the nebular phase of evolution. The most prominent emission lines are Hα (which affects R), and the Ca II triplet and [Ca II] line, which both occur in the I band. Any temperature derived from the $(V - I)$ colour index is, therefore, increasingly uncertain in this phase, and indeed, with such an extended atmosphere, the very concept of an effective temperature is starting to break down, since the envelope encompasses a wide range of temperatures, and the luminosity arises in the bulk of the material rather than at a well-defined surface.

The reduction of the observed quantities to physical parameters of the fireball is, in the absence of a detailed atmospheric model, a rather approximate procedure, particularly with regard to the derivation of the photospheric temperature. The atmosphere is electron-scattering dominated in the V to I bands, and such atmospheres are not very efficient in thermalizing the radiation field. They tend to give a higher colour temperature than the true effective temperature (Höflich, 1987; Shigeyama *et al.*, 1987). Such an effect may have been observed (Catchpole *et al.*, 1987; Catchpole, 1987; private communication). In the B and V bands, line blanketing dominates after the first week, so that the emitted flux falls well below the black-body line (Danziger *et al.*, 1987;

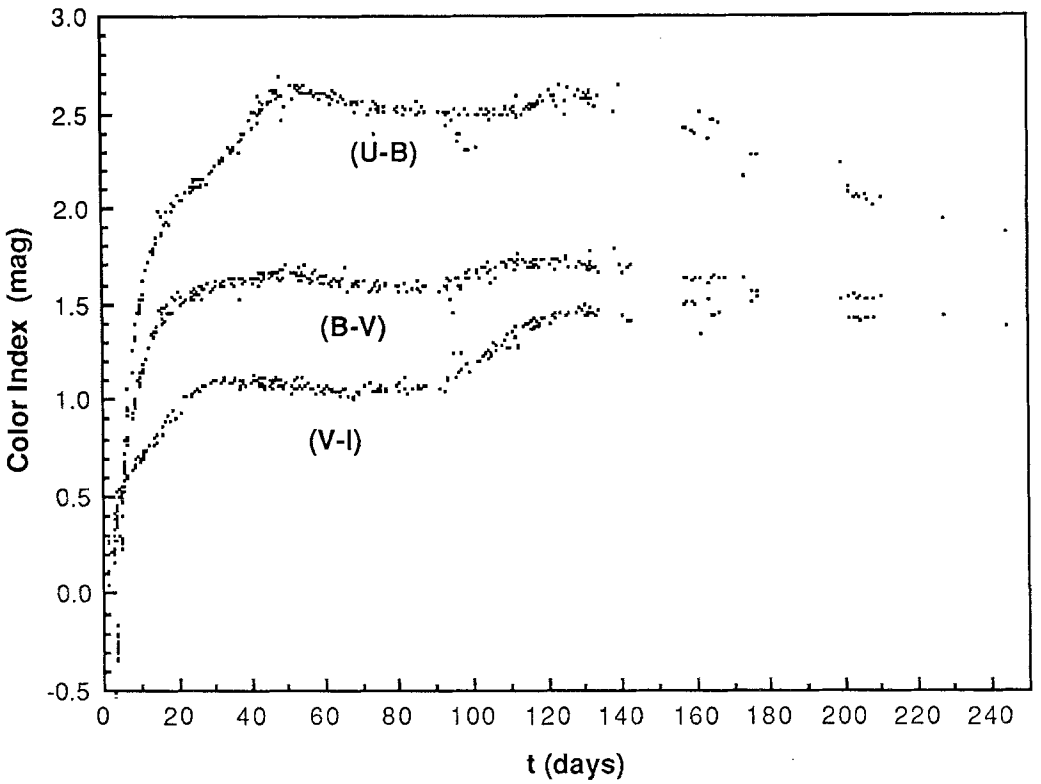

Fig. 5.2. The colour evolution of SN 1987A. Note the very rapid initial colour evolution, about five to six times faster than is characteristic of a normal Type II supernova (cf. Bartunov and Tsvetkov, 1986). This is a result of the compact nature of the precursor star.

Menzies *et al.*, 1987; Catchpole *et al.*, 1987; Hamuy *et al.*, 1987). In the L and M bands there is a pronounced excess of flux over the black-body values, and this becomes much more severe in the 8–13 μm band, as the free-free emission and opacity become dominant (Aitkin *et al.*, 1987). Alternatively, this excess may be due to an infrared echo from dust grains heated by the supernova outburst (Rank *et al.*, 1987). At late times, emission from the nebular lines becomes important, but this mainly affects R and I.

In this *Review*, we adopt the procedure described by Dopita *et al.* (1987b). The distance modulus to the LMC is taken as $(m - M)_0 = 18.5 \pm 0.1$ (Feast, 1984). An extinction of $A_v = 0.3$ and reddening of $E(B - V) = 0.11$ are used. The temperatures are derived from the $(V - I)$ colour index at late phases, and from the $(B - V)$ colour index during the first week. The temperatures so derived are about 450 K lower than those derived by Catchpole *et al.* (1987), as a consequence of the somewhat lower reddening adopted here.

The absolute luminosity is derived from the V magnitude, the distance modulus and the bolometric corrections of Carney (1980) by:

$$M_{\text{bol}} = V - (m - M)_0 + \text{B.C.} = 4.75 - 2.5 \log(L/L_\odot) \qquad (5.1)$$

and the radius from Stefan's law:

$$2\log(R/R_\odot) = 15.057 + \log(L/L_\odot) - 4\log(T_{\rm eff})\,. \tag{5.2}$$

The physical parameters so derived from these data, and all other published data are shown in Figures 5.3 and 5.4. Note the decline in both the effective temperature and

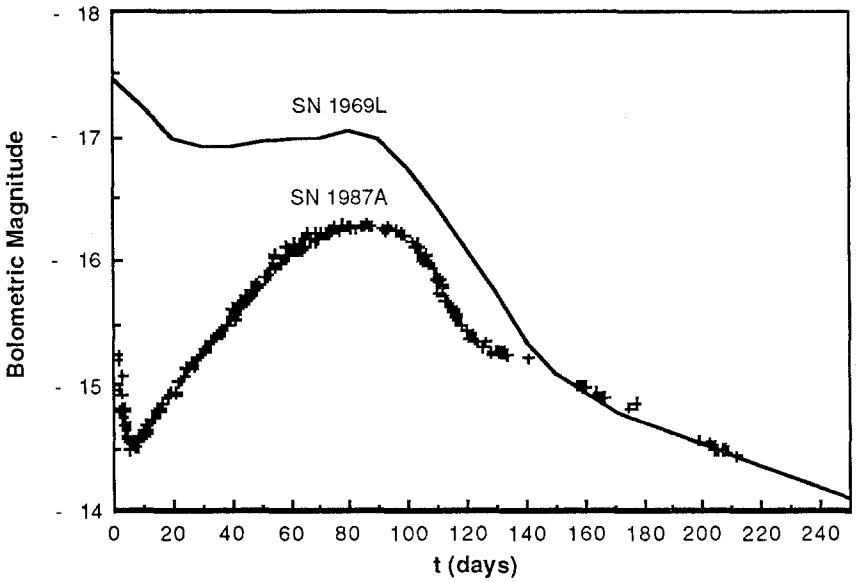

Fig. 5.3. The bolometric luminosity of SN 1987A, computed as described in the text, compared with the Type II plateau-type supernova SN 1969L (Kirshner *et al.*, 1973; Barunov and Tsvetkov, 1986). The radioactive tails coincide for an assumed Hubble constant $H_0 = 70$ km s^{-1} Mpc^{-1}. The increasing divergence of these curves at early times can be ascribed to the relatively efficient radiation of shock-deposited energy in the case of SN 1969L resulting from a more extended envelope in the precursor. Events such as SN 1987A give such a feeble optical display that they would have tended to be missed in surveys for SNe, and would also tend to be very poorly studied even if picked up.

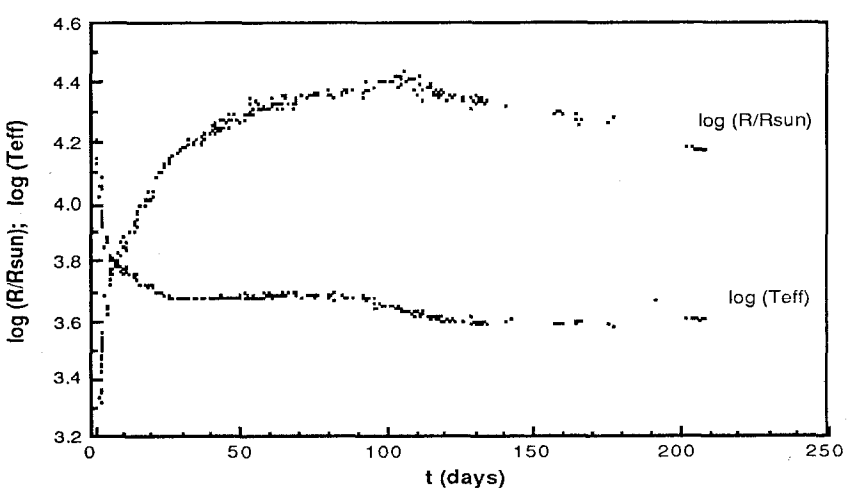

Fig. 5.4. The evolution of radius and photospheric temperature in SN 1987A, after Dopita *et al.* (1987b).

the radius of the fireball after the maximum of the light. The similarity of the later light curve with that of the Type II plateau SNe suggests a generic similarity between the core structure in SN 1987A and in the stars giving rise to such events. The luminosity in the exponential portion of the light-curve depends on the amount of radioactive material produced (see Section 7.3).

6. Spectral Evolution

6.1. Optical

The spectral evolution of SN 1987A at optical wavelengths has been intensively monitored by several groups around the world. The most complete data set in the first month is that of Hanuschik and Dachs (1987a, b). Other extensive data sets have been published by Ashoka *et al.* (1987); Danziger *et al.* (1987); Menzies *et al.* (1987); Catchpole *et al.* (1987), and Blanco *et al.* (1987). These data are all of moderately low resolution (4–8 Å), and typically cover about 3800–7400 Å. Observations have been obtained in the range 3100–7500 Å with the Anglo-Australian Telescope (AAT), generally at fairly low resolution, although a few higher resolution observations exist. The Faint Object Red Spectrograph spectra obtained at the AAT cover the range 5500–10 000 Å at a resolution of about 15 Å. These are particularly useful for monitoring the development of the Ca II triplet feature, and the [Ca II] line, relative to Hα (see Figure 6.3). A fairly extensive spectral library has been accumulated using the MSSSO 1.8 m telescope at Coudé with its 32 inch camera and the Photon Counting Array as a detector. This data has a typical spectral coverage of 3200–7400 Å, a resolution of 40 km s^{-1}, and a signal to noise of up to 100 per resolution element (see Figure 6.1). Of complete spectra, the data collected at MSSSO has the highest resolution, but has proved difficult to reduce to absolute flux.

The very earliest spectra were very smooth, but there was a very rapid development of strong Balmer lines and He I lines with very broad scattering P-Cygni profiles. Initially, the maximum expansion velocity in the absorbing material was as high as 30 000 km s^{-1}, with the absorption maximum in Hα at about 18 000 km s^{-1}. This was almost twice as large as in 'normal' Type II supernova events, and is a result of the compact nature of the precursor star. The radial velocity of the hydrogen absorption features rapidly decreased, initially by about 800 km s^{-1} each day (see Figure 6.2). This corresponds to the fastest-moving material expanding, and becoming optically thin.

The absorption velocities derived from the higher Balmer lines or Paschen lines remained systematically lower than that of Hα. The weaker lines appearing only in absorption such as Fe II λ5018 Å or λ5169 Å gave lower velocities still. This shows that the optical depth in Hα was very large indeed at the early epoch, and, therefore, that the line was formed high in the atmosphere. As we go to lines of progressively lower optical depth, we find that they are formed lower in the atmosphere with characteristically smaller radial velocities, and have line profiles which approach that of pure absorption. The weak Fe II lines mentioned above should be formed very close to the

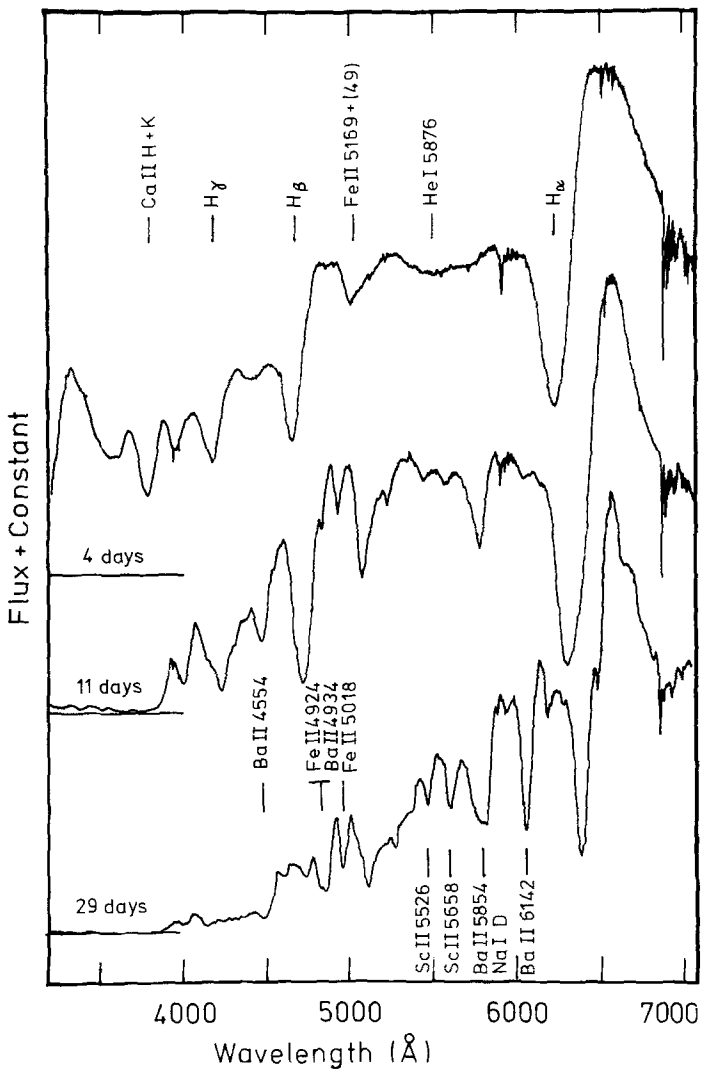

Fig. 6.1. The spectral evolution at optical wavelengths during the first month of SN 1987A. These are high resolution spectra taken at Mt. Stromlo Observatory (upper pair, courtesy of Alex Rodgers and Shaun Ryan, respectively) and at the Anglo-Australian Telescope (courtesy of Raylee Stathakis). The narrow interstellar Ca and Na lines are quite apparent. Note the very rapid redward evolution of the Balmer absorption, and the early emergence of absorption lines of *s*-process elements (see Williams, 1987). Line identifications are given with their rest wavelengths.

continuum photosphere. This conclusion is consistent with observation. On day 7 the absorption velocity in the lines was about 8000 km s^{-1} (Ashoka *et al.*, 1987; Blanco *et al.*, 1987), whilst the photospheric derived from the photometry with an assumed distance modulus of 18.5 was about 7000 km s^{-1} (Dopita *et al.*, 1987c; see Figures 6.2, 8.1). This type of comparison (Baade–Wesselink distance estimate) was used by Branch (1987a, b) an by Wagoner (1987) to estimate the distance to the LMC as 55 ± 5 kpc and 47 ± 7 kpc; respectively.

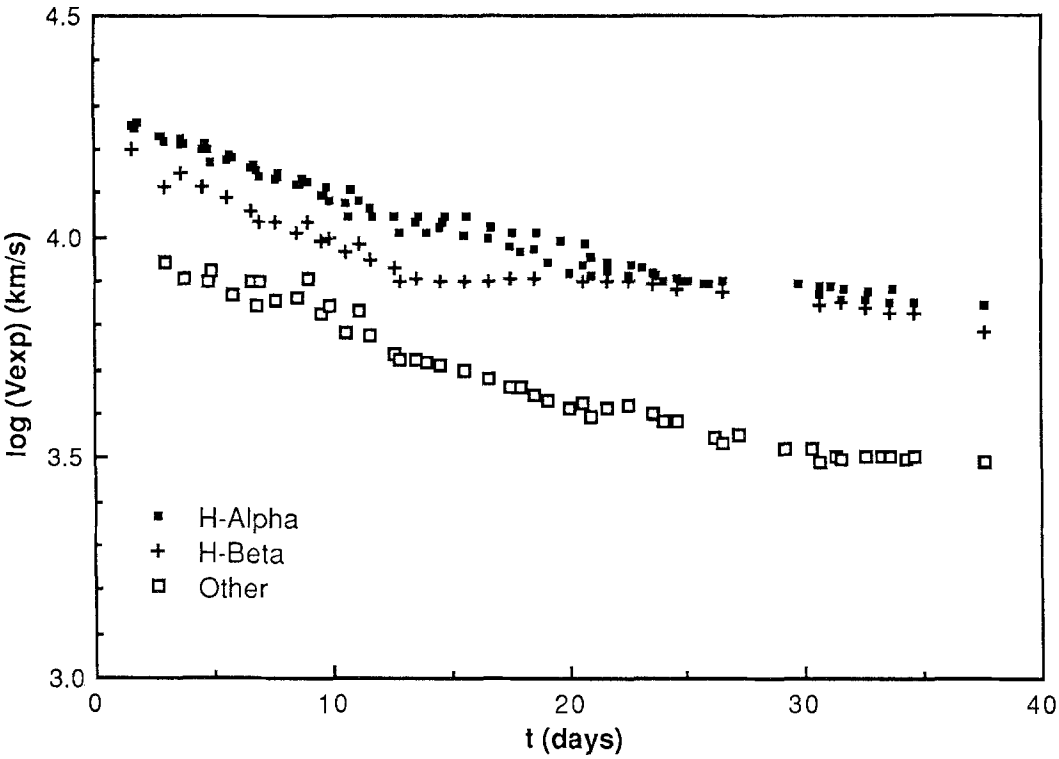

Fig. 6.2. The evolution of the absorption velocities of Hα, Hβ, and the mean of other absorption lines including Ca I at early epochs, and Na I, Fe II λ5018, and Fe II λ5169 at later epochs. Data has been taken from Ashoka *et al.* (1987), Danziger *et al.* (1987), Hanuschik and Dachs (1987), and Blanco *et al.* (1987). For comparison, the logarithm of the photospheric velocities derived from the photometric data (see Figure 7.1) are as follows: 2 d; 3.90, 10 d; 3.73, 20 d, 3.62; 30 d, 3.3.57; 40 d, 3.55. Clearly, the weaker lines give an excellent estimate of the photospheric velocity.

The Balmer lines must be formed a long way out of local thermodynamic equilibrium (LTE). Models which assume LTE fail to reproduce the observed strength of the Balmer lines after only two days, but are otherwise highly successful in describing the general spectral distribution over a decade of wavelength (Wheeler *et al.*, 1987a, b; see Figure 6.4). The occupation of the $n = 2$ state would have to be about 50–100 times its LTE value. This effect can be understood on the basis of the Höflich *et al.* (1986) or Hershkowitz *et al.* (1986) treatments of non-LTE effects is low-density electron scattering dominated atmospheres. These non-LTE effects result from four factors; the photon escape probability near the surface is very high, so that the mean intensity, $J\nu$, is reduced relative to the Planck function, $B\nu$, the radiation field is not produced locally, the sphericity dilutes the radiation field still further, and finally, the formation of spectral lines encourage deviations from LTE. Wagoner (1987) has shown that the level populations of hydrogen are governed by the balance between photoionization directly to the continuum, and by recombinations directly from the continuum. Höflich *et al.* (1986) find that in low-density atmospheres with large radii, the effects of backscattering tend

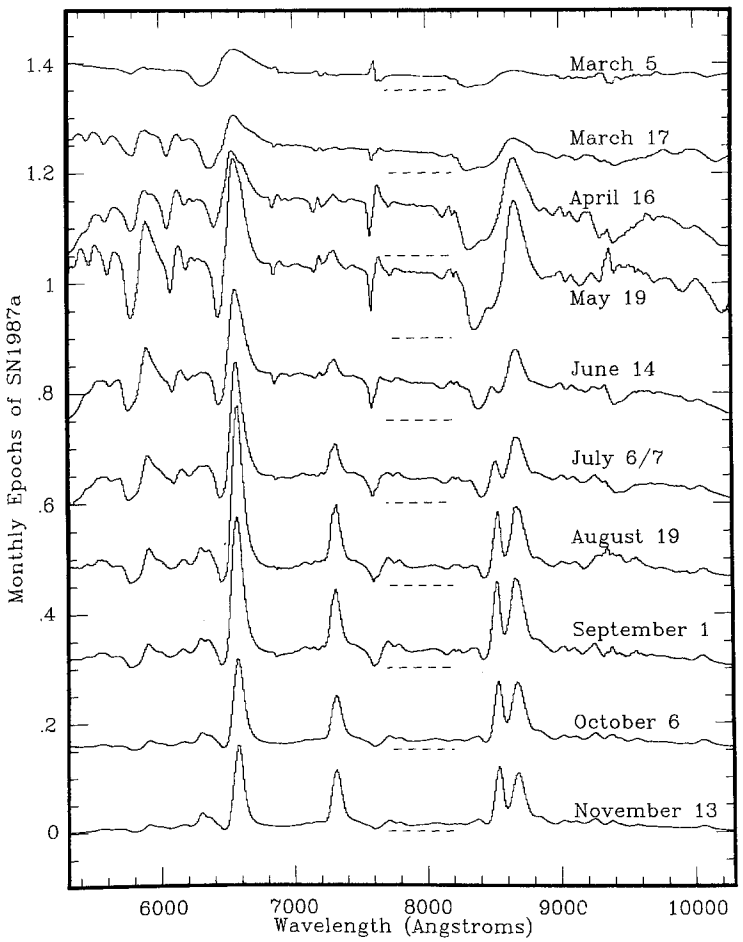

Fig. 6.3. The evolution of SN 1987A in the near infrared, showing the development of the nebular phase. This sequence was obtained using the Faint Object Red Spectrograph of the Anglo-Australian Telescope (courtesy of Raylee Stathakis of the AAO). Note how the P-Cygni Hα profile rapidly develops in emission, but the Na I feature near 5800 Å does not. The feature near 8600 Å is the Ca-triplet, and the emission feature near 7300 Å is [Ca II]. Both [O I] emission near 6300 Å, and O I absorption, near 7600 Å are visible in this sequence.

to decrease non-LTE effects. In SN 1987A, on the other hand, we are dealing initially with a compact and relatively dense atmosphere in which curvature effects certainly cannot be neglected. Thus the non-LTE effects will be very large indeed. In such an atmosphere, the electron temperature above the photosphere is roughly constant, or even increases somewhat at larger radii.

The development of a Ca II P-Cygni feature occurred very early, but by about March 3 as the photospheric temperature fell below 6000 K, and the recombination wave developed, many absorption features corresponding to Fe II, Na I, and Ti II, and other metal lines lines appeared and deepened. The general behaviour of the absorption features was fairly successfully described by Branch (1987b) for lines in the optical, UV

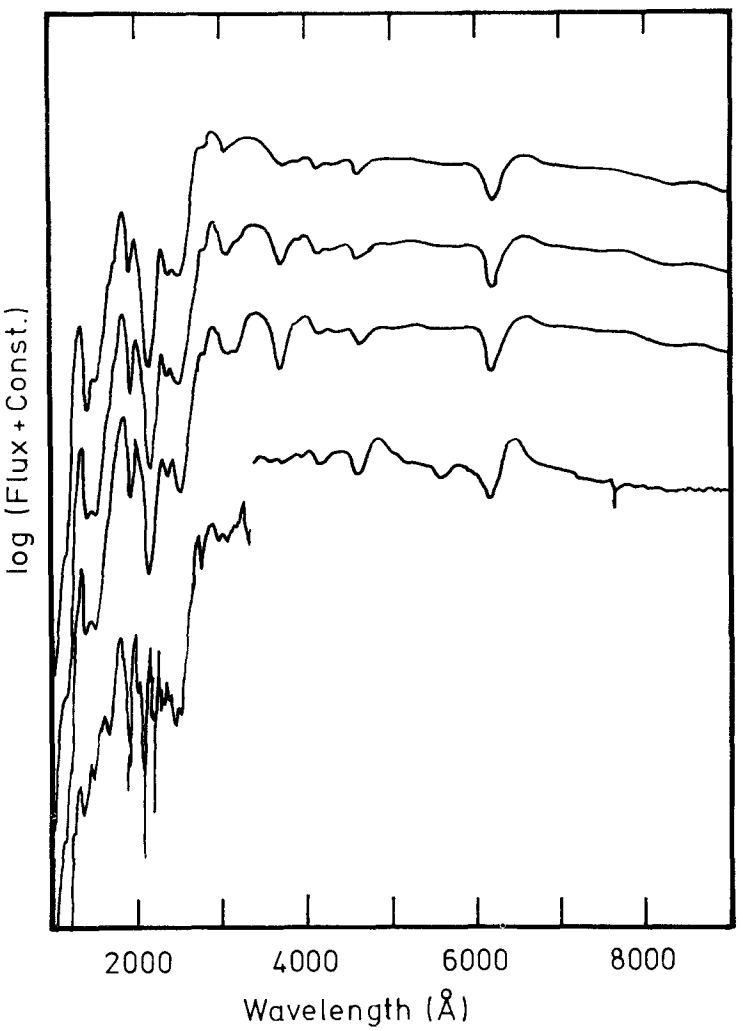

Fig. 6.4. The theoretical spectral distribution two days after the explosion (upper curves) compared with the observations at the same epoch (lower curve) (from Wheeler *et al.*, 1987b). The model atmospheres are all characterized by a power law density distribution with index-11, normalized to 1.5×10^{-14} g cm^{-3} at 20000 km s^{-1}. The three curves correspond to total luminosities of (top to bottom) 4.9, 3.9, and 3.2×10^{41} ergs s^{-1}, respectively.

and IR regions of the spectrum. He assumed an LTE optical depth in an atmosphere undergoing a differential expansion with a velocity proportional to radius. The optical depth in a line then reduces to:

$$\tau = (\pi e^2/mc) N f \lambda t (1 - \exp[-h\nu/kT]), \tag{6.1}$$

where N is the number density of absorbers in the lower level of the transition of interest, f is the oscillator strength, and t is the time since the explosion. If the electron density is known, then the LTE assumption can be used to calculate the absorber density. The density distribution in a supernova atmospheres can be approximated by a power law

with index α. For an electron-scattering dominated atmosphere, the electron density at the photosphere, n_e, is given by:

$$n_e = (\alpha - 1)/\sigma_e R\,, \tag{6.2}$$

from which the optical depth in the various lines may be calculated. It might be considered somewhat curous that the LTE approach is rather successful for the metal lines, given our discussion above about the hydrogen lines. In fact, non-LTE effects will occur, but are much less serious for the metal lines, since, as already stated, these are formed close to the photosphere.

As the metal lines appeared and deepened, intense absorption lines of the *s*-process elements Ba and Sc appeared (see Figure 6.1). These are particularly interesting, and may indicate real enhancements of the abundances of these elements in the outer layers (Williams, 1987). Normally, one would expect these elements to be produced in the He-burning layers, so an overabundance would indicate a considerable degree of mixing, either in the pre-supernova star, or else in the supernova fireball itself. However, again, one must beware of non-LTE effects and treat such abundance estimates with caution.

Throughout the second half of March and through April, the rate of spectral evolution slowed considerably. Line blanketing below 4400 Å became almost total, and the depth and width of the absorption lines continued to decrease slowly. During this period, pronounced irregularities appeared in the Hα profile (Hanuschik and Dachs, (1987a, b). These consisted of a pronounced oscillation in the transition region between the absorption trough and the maximum of the emission, and a bump on the redward side of the emission feature. This may have been an indication of deviations from a spherically-symmetric outflow. These features faded and finally disappeared during April.

The Hβ line showed a particularly interesting behaviour. This reached a maximum in absorption by about March 8 (Hanuschik and Dachs, 1987a, b) before almost disappearing during April. However, it returned to become a prominent and almost saturated absorption line in late June, and higher members of the Balmer series became clearly visible once again (see Figure 6.5). By late October, the depth of the absorption was decreasing as the line developed in emission. What could have caused the initial fading of Hβ and its subsequent return? This may have been the effect of veiling by the Fe II features according to Chugaj (private communication). This interpretation would imply that these lines were all being produced in the same portion of the atmosphere. A second possibility is that, as the atmosphere expanded, the $n = 3$ level of hydrogen approached its LTE population as a result of the lower density, greater photospheric radius and the increasing importance of backscattering. This seems, on balance, to be the most reasonable hypothesis. A third possible explanation is that hard X-rays started to heat the layers above the photosphere leading to an increase in the excitation temperature of the hydrogen.

The re-emergence of the Hβ lines heralded the onset of the nebular phase, with Hα and Ca II developing in emission and [Ca II] emission appearing near λ7400 Å. The ratio of the Ca II to [Ca II] emission will provide a very useful density diagnostic. The

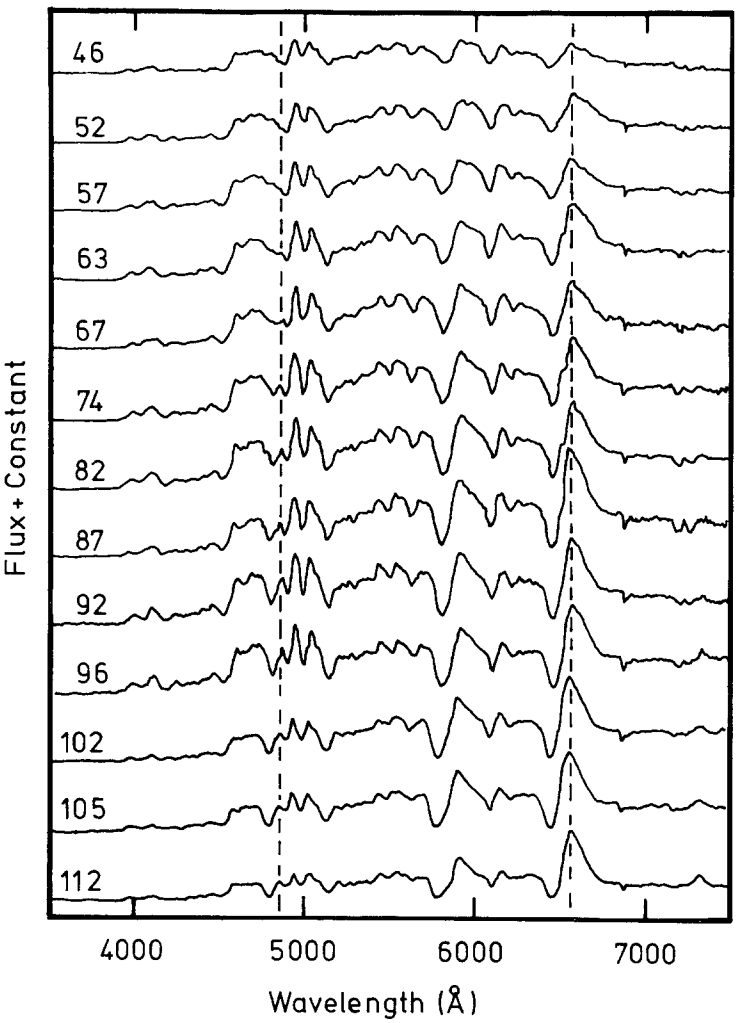

Fig. 6.5. The evolution of the optical spectra to the onset of the nebular phase, taken from Catchpole *et al.* (1987). The rest wavelengths of Hα and Hβ are shown by dotted lines. Note the extreme weakness of Hβ absorption at the start of this sequence, followed by its re-emergence at about day 70.

O I λ7774 Å feature also appeared in absorption for the first time at the start of the nebular phase in June, suggests that oxygen-rich material may have first reached the photosphere at this epoch. By the beginning of December the [Ca II] line was approaching Hα in intensity, and forbidden lines of other elements such as [O I] λ6300, 6363 Å and λ5577 Å were visible. These lines can be expected to permit an independent determination of the evolution of the electron density, or of the electron temperature at sufficiently late time. The nebular phase is discussed further below.

As pointed out by McCall (1984), the polarization spectrum of a supernova carries information on the physical processes occurring during the outburst. In particular, as a result of the dominance of electron scattering, any asymmetry in the shape of the

fireball will manifest itself as a non-zero net polarization. If the atmosphere is non-spherical then the distances calculated by the Baade–Wesselink method (which assumes a spherical expansion) will be incorrect. Within spectral lines, resonance scattering will introduce a wavelength-dependent polarization. This provides additional constraints on the distribution of absorbers and the density structure within the atmosphere.

Polarimetric data on SN 1987A has been reported by Schwartz and Mundt (1987), but much more extensive monitoring has been carried out on the Anglo-Australian telescope by Cropper *et al.* (1987) (see Figure 6.6). The initial continuum polarization was about 0.8%, but this subsequently decreased. However, the polarization in the lines, particularly in the absorption component of Hα has increased sharply. Since the polarization is determined by the interstellar dust, the shape of the supernova fireball and the scattering processes in the photosphere, these results are difficult to interpret until we have reliable estimate of the intestellar polarization towards SN 1987A. However, both Jeffery (1987) and Cropper *et al.* (1987) have made some progress in the

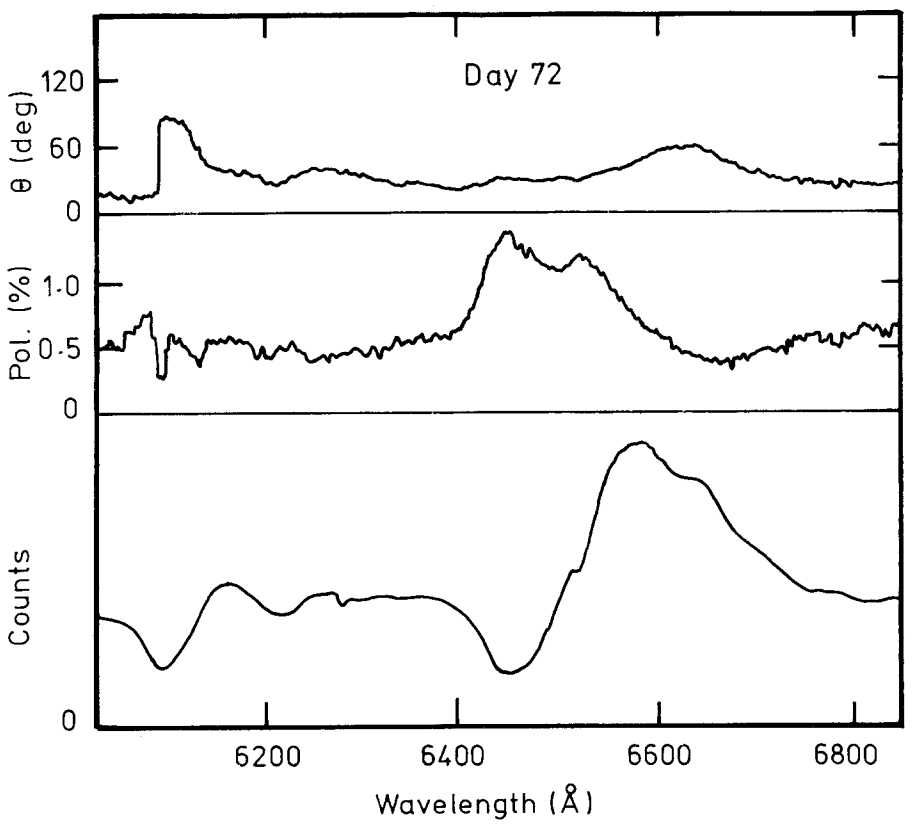

Fig. 6.6 The polarization in the vicinity of the Hα and the Na-D lines some 72 days after the explosion (from Cropper *et al.*, 1987).

interpretation of these results. The wavelength dependence and time variability of the broadband polarizations, and the existence of strong features across lines in the polarization spectrum, are all strong indicators of the existence of some intrinsic asphericity in the supernova fireball. Jeffery estimates that the ratio of the symmetry axis to the perpendicular axis (c/a) was (c/a) $\sim$ 0.6–0.8 in early March. From their data set, Cropper *et al.* (1987) find (c/a) = 0.93 at the same epoch, but that it decreases to about 0.88 at later times. There is some evidence that the departures from sphericity are also wavelength dependent. When the Baade–Wesselink method is used on the assumption of spherical expansion, errors of the order of $(c/a)^{-1/2}$ in the distance will result. This would indicate that, for example, the Branch (1987a) distance estimate of 55 $\pm$ 5 kpc should be reduced to about 52 $\pm$ 5 kpc, and the Wagoner (1987) distance of 47 $\pm$ 7 kpc should be reduced to 45 $\pm$ 7 kpc. The average of these, 50 $\pm$ 5 kpc is in excellent agreement with recent estimates for the distance to the LMC based on other techniques (50 kpc; Feast, 1986).

6.2. Ultraviolet

The IUE observations began at 19 : 00 UT on 24 February 1987, just 14 hours after Shelton's discovery, and the initial results have been described by Wamsteker *et al.* (1987), Cassatella *et al.* (1987a, b), and Kirshner *et al.* (1987). A remarkable feature of the earliest spectrum is the existence of an enormously broad Mg II P-Cygni scattering feature. This feature shows a 'photospheric' velocity of about 20 000 km s^{-1} with material apparent up to about 35 000 km s^{-1}. If this identification is correct, then the absorption dip near 1530 Å may be the He II λ1640 Å resonance line. The prominent absorption dip at 1700–1800 Å would then be due to lines in the λ1840–1910 Å region. This is almost certainly identified with the Al III doublet at λ1855.63 Å (Lucy, 1987). The sharp drop and termination of the February 26 spectrum below λ1316 Å is due to strong line blocking by Si II, Si III, and S II (Lucy, 1987). An excellent fit between the observed and computed spectral distributions is displayed by the LTE/relativistic expanding atmosphere calculations of Wheeler *et al.* (1987b; see Figure 6.4) or Spies *et al.*, 1987a, b).

Within 4 days the flux in the IUE short wavelength region declined *one thousand-fold*, leaving only an apparent emission line feature just below 1900 Å. At longer wavelengths, the spectra taken on February 27–28 are almost identical to the 'classical' Type I SN, SN 1980N in NGC 1316, and SN 1981B in NGC 4536 (Panagia, 1985). Both this superficial similarity with Type I events, and the very rapid decline in the UV flux can be explained as a result of the anonymously low temperature achieved in this supernova within a very few days of the event. This resulted in almost complete UV blanketing by over 200 lines of heavy elements such as Fe and Ni in their second or third ionization stages (Lucy, 1987; Wheeler *et al.*, 1987a, b). The 'emission' feature at 1900 Å is simply a gap in the otherwise complete UV black-out.

From about mid-May, the UV emission started to increase once more as the line blocking decreased. This and later phases were marked by the appearance of a set of narrow emission lines mainly due to nitrogen, which may indicate the photoionization

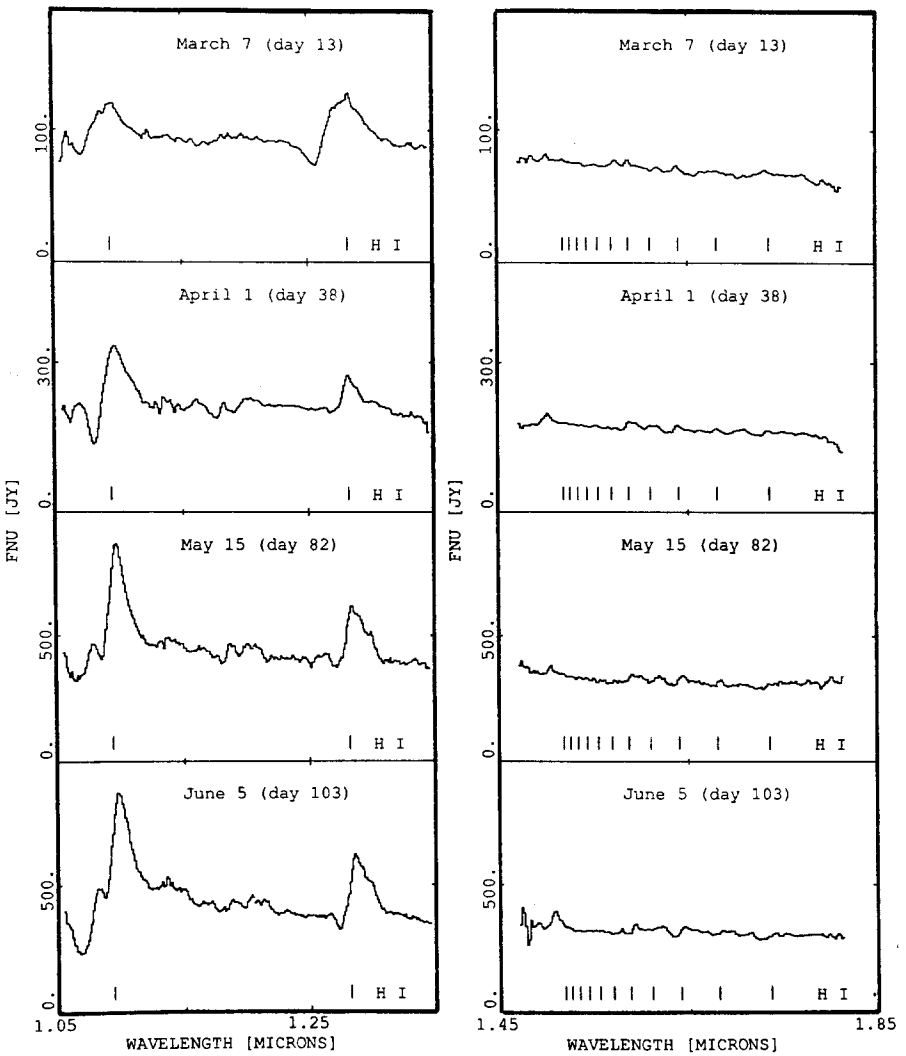

Fig. 6.7. Near-infrared spectra (1.05–1.35 and 1.45–1.85 μm) obtained at MSSSO using the CIGS spectrograph (courtesy of Peter McGregor). The main hydrogen features are marked, and other emission lines are identified in the text.

of the circumstellar material ejected in the pre-supernova phase (Kirshner, 1987; see Figure 8.1 and Section 8).

6.3. Infrared

Regular spectral monitoring has been carried out in the IR at MSSSO, between 1.0–1.4, 1.45–1.85, 1.9–2.5, and 2.9–4.1 μm (McGregor *et al.*, 1988) and at the AAO by Allen in the same wavelengths, but also at 8–13 μm (Aitken *et al.*, 1988). The monitoring at MSSSO has been performed at approximately monthly intervals since core collapse, and the results of this are shown in Figures 6.7–6.11. The spectrum has evolved from

a relatively featureless continuum with a few broad P-Cygni lines of hydrogen of the Paschen, Brackett, and Pfund series, to a rich emission-line spectrum with features reminiscent of a nova. The near-infrared continuum is a smooth extrapolation of the electron-scattering dominated optical continuum, with a temperature or order 4500 K during most of the period of monitoring. The continuum distribution in the 8–13 μm band, on the other hand, is consistent with the opacity being dominated by the free-free contribution.

On day 13, the maximum blue-shifted absorption in the infrared hydrogen lines was $\sim 11\,000$ km s^{-1}, compared with $\sim 17\,000$ km s^{-1} in Hα on the same date. This difference is to be expected, since the scattering optical depth in the infrared lines is

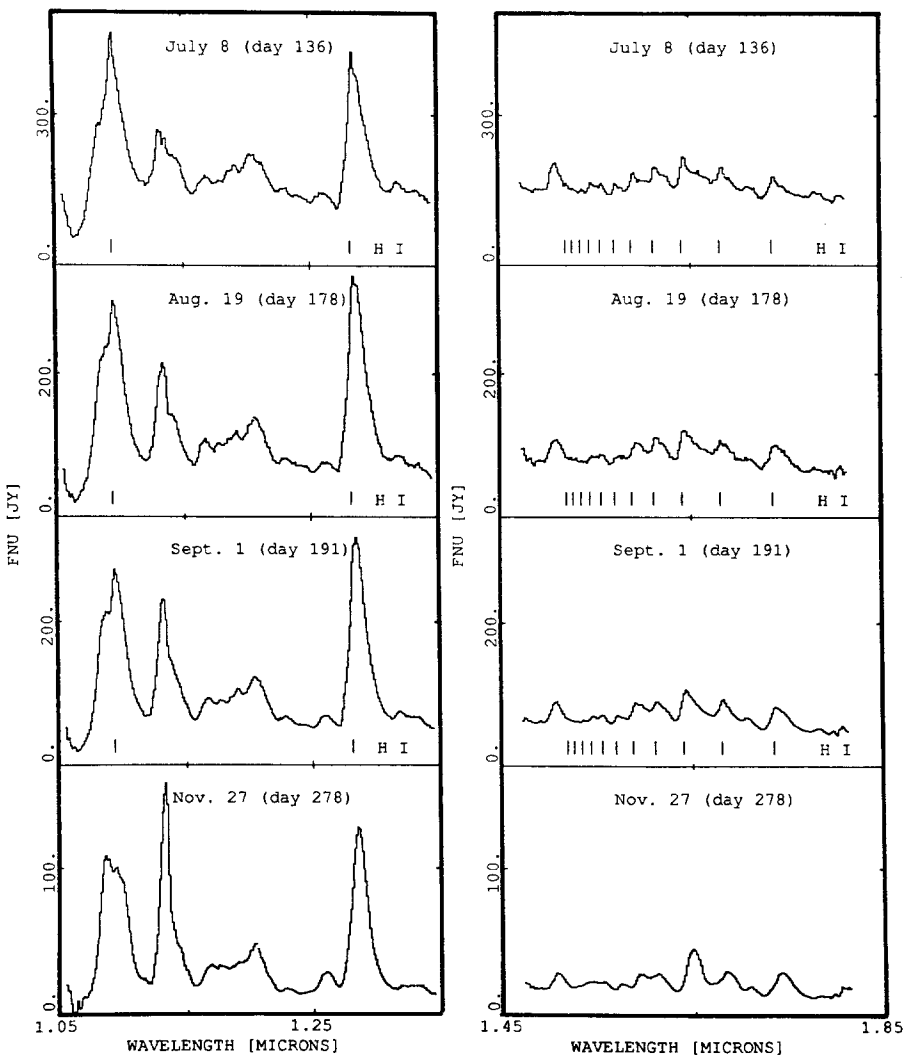

Fig. 6.8 As Figure 6.7, but into the nebular phase of evolution. The many hydrogen emission lines, and the structure of the other emission features (identified in the text) are very reminiscent of a nova.

smaller. After day 82, the velocity of the absorption minimum in the Pβ line remained constant at about 2300 km s^{-1} while becoming shallower. This velocity probably indicates the velocity of the densest layers closest to the photosphere and, therefore, probably represents the lowest velocity of ejection in the hydrogen-rich envelope.

Apart from the hydrogen lines, a variety of lines of other ionic species have been identified. The feature which appeared at about 1.066 μm on day 38, and which has strengthened into a P-Cygni profile blended with the Pγ line may be the He I $2^3P - 2^3S$ at 1.083 μm. The Pγ feature itself is probably a blend, since it exceeds the strength of Pβ for intermediate epochs. It may be blended with the [Si I] 1.0991 μm feature, which

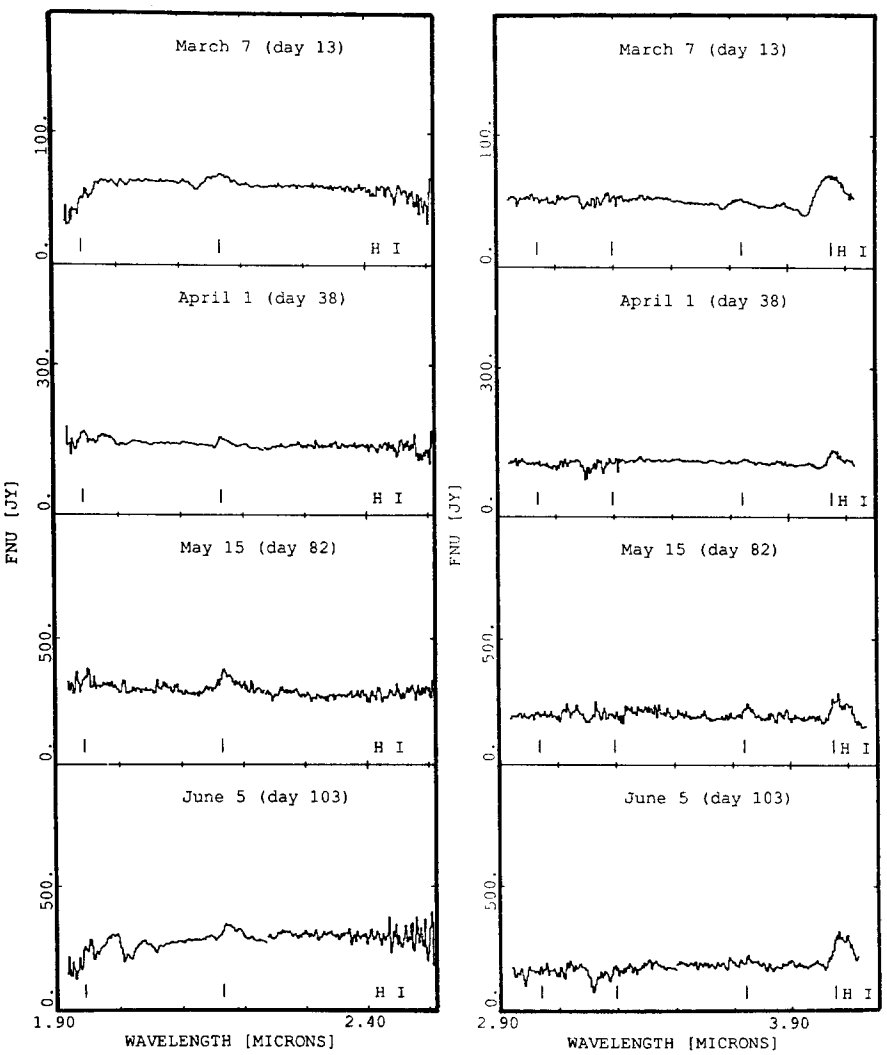

Fig. 6.9. Near-infrared spectra (1.90–2.50 and 2.90–4.05 μm) obtained at MSSSO using the CIGS spectrograph (courtesy of Peter McGregor). The main hydrogen features are marked, and other emission lines are identified in the text.

is predicted to be strong in the Si–Ca zone of ejecta (Fransson and Chevalier, 1987; see also Section 7). The strong feature at 1.13 μm is either O I 1.128 μm or C I 1.133 μm. The complex emission structure between 1.16 and 1.22 μm is almost certainly a blend of C I and Si I lines.

A particularly interesting discovery was the development of the first overtone band of CO in emission after about 120 days. The lines are broad, and the intensity of the emission is consistent with the hypothesis that it is produced by collisional excitation in optically thick conditions at densities of the order of $10^9\,\mathrm{cm}^{-3}$ in or near the photosphere. The CO gas is probably formed by direct chemical association as the carbon- and oxygen-rich products of helium-burning flow over the photosphere. The

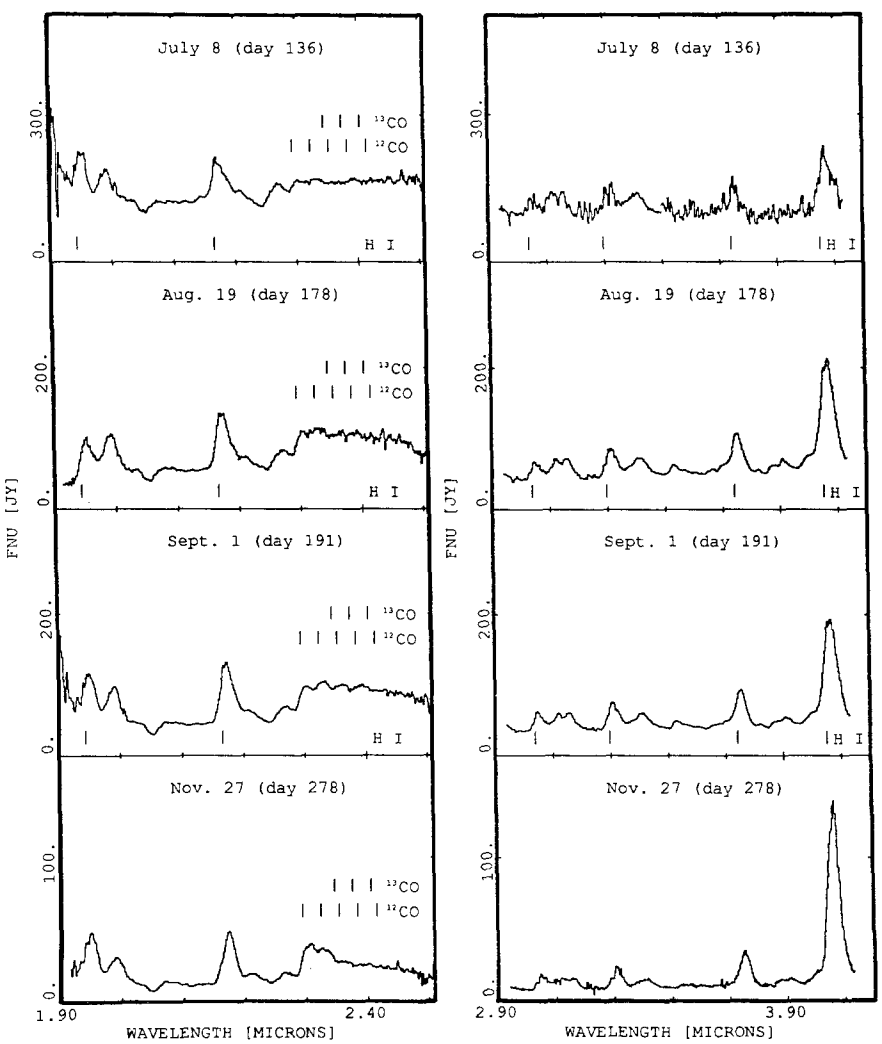

Fig. 6.10. As Figure 6.9, but during the nebular phase of evolution. Note the development of CO in emission, and the decrease in the excitation temperature apparent at the later epochs.

latest spectra are becoming strongly peaked at the 2–0 bandhead. This suggests a lowering of the vibrational temperature below ~ 3000 K. CO emission in its fundamental vibration-rotation band is responsible for an excess seen in the M band (4.55–5.00 μm) seen in photometric data.

7. Later Phases of Fireball Evolution

7.1. The hydrogen recombination wave

After $t = 5$ days, the rate of expansion slowed markedly, and the temperature stabilized as a hydrogen recombination wave started to propagate inwards. As this occurs, the luminosity of the supernova is derived from the (adiabatically degraded) internal energy (Woosley, 1987). Initially, the photosphere and the recombination wave move inwards together. However, Dopita (1987a, b) has shown that, as the inward velocity of the recombination wave increases, the residual opacity of the overlying layers becomes more and more important, until eventually the photosphere is left behind.

This will have important effects on the light curve, since the internal energy released as the recombination wave moves in towards the core cannot be immediately radiated, but instead will have to diffuse out through the low temperature region between the recombination front and the photosphere. This will have the effect of smoothing out the variations in the light curve, lowering the photospheric temperature and delaying the release of the shock-deposited energy. This effect could go a long way towards explaining the discrepancy between the smooth form of the observed light curve, and those derived from models (Nomoto *et al.*, 1987; Woosley *et al.*, and Ensman 1987a; Woosley, 1987), which all show pronounced oscillations at early times (see Figure 7.2).

7.2. To maximum light

After the recombination front has disappeared below the photosphere, by about $t = 20$ days, the evolution to the maximum luminosity occurred at an almost constant photospheric temperature. We can, therefore, regard the material which passed over the photosphere between 20 and 90 days as having a constant degree of ionization. If we can assume that the shocked SN ejecta has a homologous expansion, and that locally, the density structure can be represented by a power law with index α, then it follows that the evolution of the radius of the fireball, R, also follows a power law, $R \propto t^{(\alpha-3)/(\alpha-1)}$. Thus, from the slope of the $\{\log(R); \log(t)\}$ relationship, we can directly derive the index of the density gradient at the photosphere (e.g., Branch, 1987a, b).

Following the disappearance of the recombination wave below the photosphere at about $\log(t) \sim 6.1$, the pre-maximum $\{\log(R); \log(t)\}$ relationship can be approximated by three such power-law segments (Figure 7.1);

$$6.10 < \log(t) < 6.35\,, \quad \alpha = 10.6 \pm 1.5\,;$$

$$6.35 < \log(t) < 6.60\,, \quad \alpha = 5.1 \pm 0.20\,;$$

$$6.60 < \log(t) < 6.95\,, \quad \alpha = 4.1 \pm 0.15\,.$$

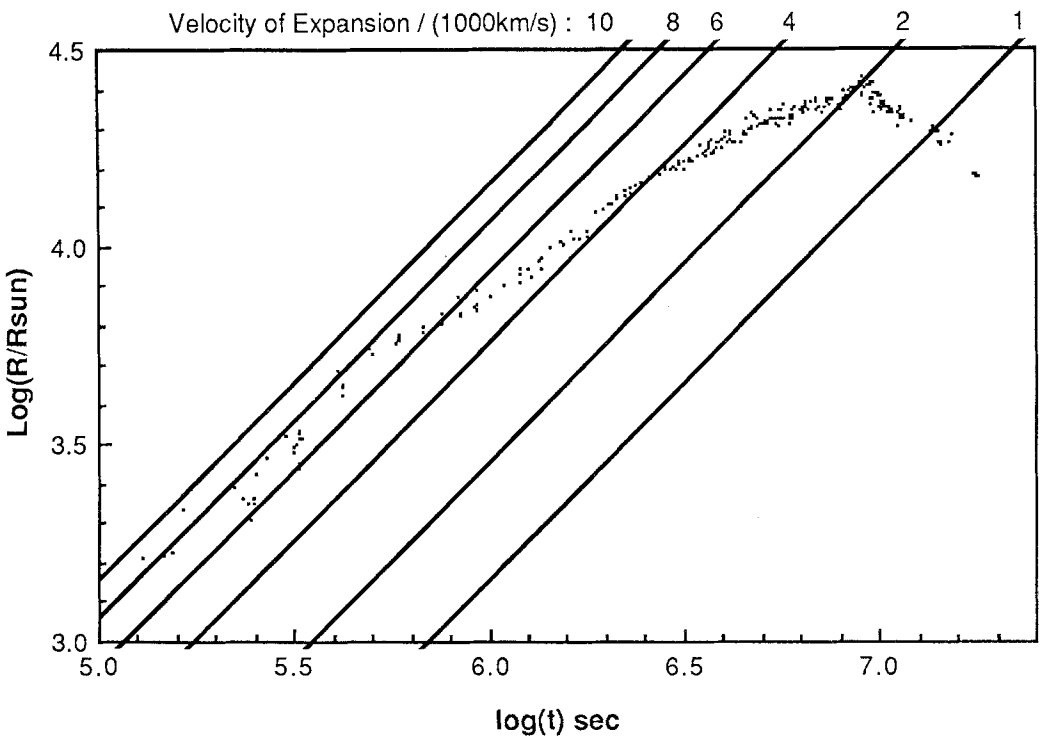

Fig. 7.1. The evolution of the photospheric radius with time. The lines are for constant velocities of expansion since the explosion, as indicated on the top of the figure.

These figures put important restraints on the structure of the pre-supernova star. They both define the density structure in the exploded star, following the passage of the shock, and allow an estimate to be made of the mass of the ejecta, provided that a scaling density can be found.

Woosley (1987) has shown that an important constraint on the hydrogen mass estimate can be established by determining dynamically the lowest velocity of ejection. The infrared lines give the lowest value for this quantity, and they ought to be the most reliable because the optical depth in these lines is least. From spectra taken by P. McGregor (Figures 6.7–6.11) at 104, 136, and 178 days, we find that the Pβ line gives minimum absorption velocities of 2220, 2520, and 2320 km s^{-1}, respectively. From Figure 7.1, this corresponds to the last of the hydrogen coming through the photosphere at $\log(t) = 6.85 \pm 0.05$ s. From the Woosley (1987) models this velocity corresponds to a hydrogen envelope mass of $5 \pm 2\,M_\odot$ for high-energy explosions ($E_{kin} = 1.4 \times 10^{51}$ ergs), or $3 \pm 1\,M_\odot$ for low-energy explosions ($E_{kin} = 6.5 \times 10^{50}$ ergs). This is entirely consistent with the Nomoto *et al.* (1987) estimate of $6.7\,M_\odot$ at an explosion energy of $E_{kin} = 1.5 \pm 0.5 \times 10^{51}$ ergs, and also with the Dopita (1987a, b) estimate of $5\ (+7; -3)\,M_\odot$ derived by direct integration of the observed density profile given above. It is clear, therefore, that energetic considerations restrict the hydrogen mass in the range of $3–8\,M_\odot$. To obtain a self-consistent intermediate

mass such as this would require the hydrogen-rich envelope to be somewhat enriched in helium (Barkat and Wheeler, 1988; Wheeler *et al.*, 1987b).

The timing of the maximum in the light curve is determined by the diffusion processes. The trapped energy of the fireball is lost at a time, t_m, when the diffusion time-scale, t_d, is comparable with the hydrodynamic time-scale, t_h:

$$t_m = (2t_d t_h)^{1/2} . \tag{7.1}$$

The diffusion time-scale is given by $t_d = 3\kappa R^2/\alpha V_{\exp} c$, where κ is the opacity, α is a structure constant, $V_{\exp}$ is the expansion velocity, and c is the speed of light. The hydrodynamical time-scale is simply $t_h = R/V_{\exp}$. Schaeffer (1987a) gives the following useful analytic approximation to the time-scale t_m in terms of the explosion energy and mass ejected;

$$t_m = 7 \times 10^6 [E_{\text{kin}}/10^{51} \text{ ergs}]^{-1/4} [M/10\, M_\odot]^{3/4} \text{ s} . \tag{7.2}$$

About 4–5 $M_\odot$ of helium and heavy elements was ejected, whereas about 3–8 $M_\odot$ of hydrogen was thrown off. Equation (7.2), therefore, defines E_{kin} to lie in the range

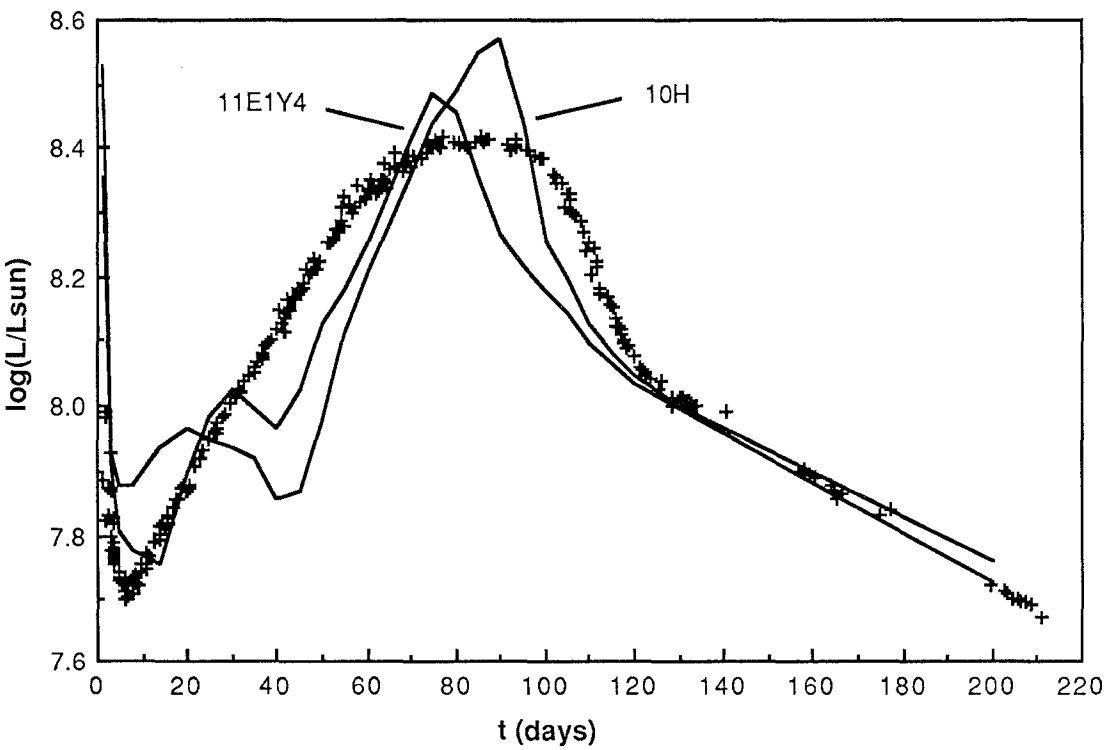

Fig. 7.2. A comparison of the observed light curve with two representative theoretical light curves from the literature. The curve marked 10H is from Woosley (1987) and has an envelope mass of 10 $M_\odot$ with an explosion K.E. of 1.4×10^{51} ergs. The model marked 11E1Y4 is from Nomoto *et al.*, and has an envelope mass of 6.7 $M_\odot$ and an explosion energy of 10^{51} ergs. The differences between the models and observations will probably reduce with a better treatment of opacity, of the recombination wave and of mixing of the radioactive Ni.

$0.5–2.0 \times 10^{51}$ ergs, essentially the same range defined by detailed computations of the light curve (Woosley, 1987a, b; Shigeyama *et al.*, 1987; see Figure 7.2).

7.3. The radioactive tail

The opacity of the core is determined by electron scattering. As oxygen and neon, the most abundant heavy elements contained in the core recombine, the opacity declines precipitately and the diffusion time-scale rapidly decreases (Schaeffer *et al.*, 1987; Schaeffer *et al.*, 1987b). This allows the stored heat energy to drain away. As the temperature falls, the recombination becomes still more rapid. Thus the core rapidly transforms itself from a condition in which the diffusion time-scale is much longer than the dynamical time-scale, to a condition in which the reverse is true. The luminosity in this latter phase can be set equal to the rate of energy generation in radioactivity (Weaver *et al.*, 1980):

$$L = 3.9 \times 10^9 \exp[-t/\tau_{Ni}] + \\ + 7.03 \times 10^9 \{\exp[-t/\tau_{Co}] - \exp[-t/\tau_{Ni}]\} \text{ erg g}^{-1} \text{ s}^{-1} . \quad (7.3)$$

where $\tau_{Ni} = 8.80$ days and $\tau_{Co} = 113.7$ days are the respective decay times on radioactive nickel and cobalt. Provided that this phase is reached in a time appreciably greater than τ_{Ni}, the luminosity will decline exponentially with a time constant τ_{Co}, until the core starts to become transparent to the parent γ-rays.

The observations (Figure 5.1) show that this phase is fully reached by $t = 130$ days, and continued up to 280 days. In this phase the V magnitude fits to a relation of the form:

$$V = 3.106 \pm 0.026 + 9.907 \pm 0.165[t/1000 \text{ days}]$$

and the luminosity is given by

$$\log(L/L_\odot) = 8.538 \pm 0.007 - 4.033 \pm 0.041(t/1000 \text{ days}] .$$

These relations correspond to exponential decay time-scales of 109.6 ± 1.9 days and 107.7 ± 1.1 days. These figures are both slightly shorter than the 113.7 day time-scale of the radioactive cobalt decay, but in view of the fact that the temperature is so uncertain in this phase, this difference is unimportant.

At $t = 127$ days, the luminosity due to radioactivity was $\log(L/L_\odot) = 8.00 \pm 0.15$. This corresponds to $0.085 \pm 0.029\ M_\odot$ of radioactive nickel having been produced in the original explosion. This figure has important implications for the chemical evolution of galaxies. The models of the progenitor and the subsequent explosion show that $1.7 \pm 0.3\ M_\odot$ of oxygen were produced. This corresponds to an [O/Fe] $= 0.65 \pm 0.25$. This is very similar to the asymptotic value observed for extreme Population II halo stars in the Galaxy; [O/Fe] $= 0.7 \pm 0.2$ (Sneden, 1985; and references therein). Therefore, to the extent that one believes that SN 1987A represented a typical Type II event, the implication is that Type II supernova events dominated the nucleosynthesis in the collapse phase of our galaxy. The [O/Fe] value falls towards solar only as the iron

produced in the Type I carbon deflagration events became important. Provided that the time delay after which this occurs is sufficiently long (comparable with the collapse time-scale of the proto-Galaxy), it is not necessary to introduce additional assumptions such as, for example, a change in the initial mass function or the existence of super-massive stars, to explain the halo [O/Fe] ratio.

7.4. The escape of X-rays and γ-rays

X-rays or γ-rays can be produced either from radioactive products produced within the supernova, or from an embedded pulsar (McCray *et al.*, 1987). Up to the time of writing, the first alternative appears to be the major source of the late luminosity of SN 1987A. The radioactive energy from Co-decays is produced in the form of γ-rays with energies in the range 0.511 up to 3.452 MeV (Gehrels *et al.*, 1987), and with a total luminosity given by Equation (7.3). Initially, all this energy is absorbed in the material surrounding the radioactive core and down-converted by repeated scatterings to the optical, as described above. As the fireball expands, the optical depth to the Co-rich central core declines and the γ-rays eventually start to leak out. The Compton-scattered γ-ray lines form a hard X-ray continuum which fades and hardens as the core becomes transparent. Several groups have already published theoretical calculations based on this scenario (Gehrels *et al.*, 1987; Grebenev and Sunyaev, 1987; McCray *et al.*, 1987; Itoh *et al.*, 1987; Pinto and Woosley, 1987; Shull and Xu, 1987; Xu *et al.*, 1987). As pointed out by Woosley *et al.* (1987a), the peak γ-ray flux is determined by the competition between the decreasing opacity of the core, and the depletion of the radioactive material. The escape probability of a γ-ray photon is approximately $\exp[-\tau]$, where τ scales as t^{-2}. The amount of ^{56}Co declines as $\exp[-t/t_{\mathrm{Co}}]$ where $t_{\mathrm{Co}} = 113.7$ days. The time of maximum γ-ray luminosity is, therefore:

$$t_{\max} \approx [2\tau_0 t_0^2 t_{\mathrm{Co}}]^{1/3}\,, \tag{7.4}$$

where τ_0 is the optical depth to the Co-rich layers at time t_0. From a simple model with homologous expansion at velocity V_4, in units of 10^4 km s^{-1}, Shull and Xu (1987) show that an optical depth of unity for Thompson scattering is reached when $t = 148[M/M_\odot]^{1/2}\, V_4^{-1}$ days. Thus, from Equation (7.4);

$$t_{\max} \approx 171[M/M_\odot]^{2/3}\, V_4^{-1/3}\,. \tag{7.5}$$

This equation indicates the essential physics of the problem. High-energy, low-envelope mass explosions will produce an early and bright γ-ray signature and *vice versa*. Taken in conjunction with the X-ray observations, γ-ray line data will provide a very useful constraint on models.

The X-rays will reach a maximum when then optical depth for scattering is just sufficient to Comptonize the γ-rays to X-ray energies. The fractional change in energy in each scattering is of order $\Delta E/E \approx -(E/m_e c^2)$. Thus, for a random walk, 20 keV X-rays will emerge after some 25 scatterings, or at a core optical depth of about 5. Thus the X-ray luminosity will peak at about 40% of the time of the γ-ray maximum.

The discovery of the hard X-ray emission by the *Ginga* satellite (Dotani *et al.*, 1987), and by the 'Röntgen' observatory in the *Kvant* module of the MIR space station (Sunyaev *et al.*, 1987) allows a direct test of theory. The first positive detection by *Ginga* was in early July, and the flux in the 10–30 keV band rose steadily to a peak in early September. The *Kvant* observations were made with three instruments, the High-Energy X-ray Experiment (HEXE), which made the initial detection, the Coded Mask Imaging Spectrometer (TMM), which has a resolution of 1.8 arc min, and the Pulsar X-1 instrument. These instruments together cover the 10–1000 keV band. The X-ray spectrum defined by these observations is extremely hard, with a power law index of about -2 below 10 keV and about -1.4 at higher energies (see Figure 7.3).

It seems likely that the bulk of the X-ray flux below 10 keV can be accounted for by thermal bound-bound, bound-free, free-free, and two-photon continua originating in the

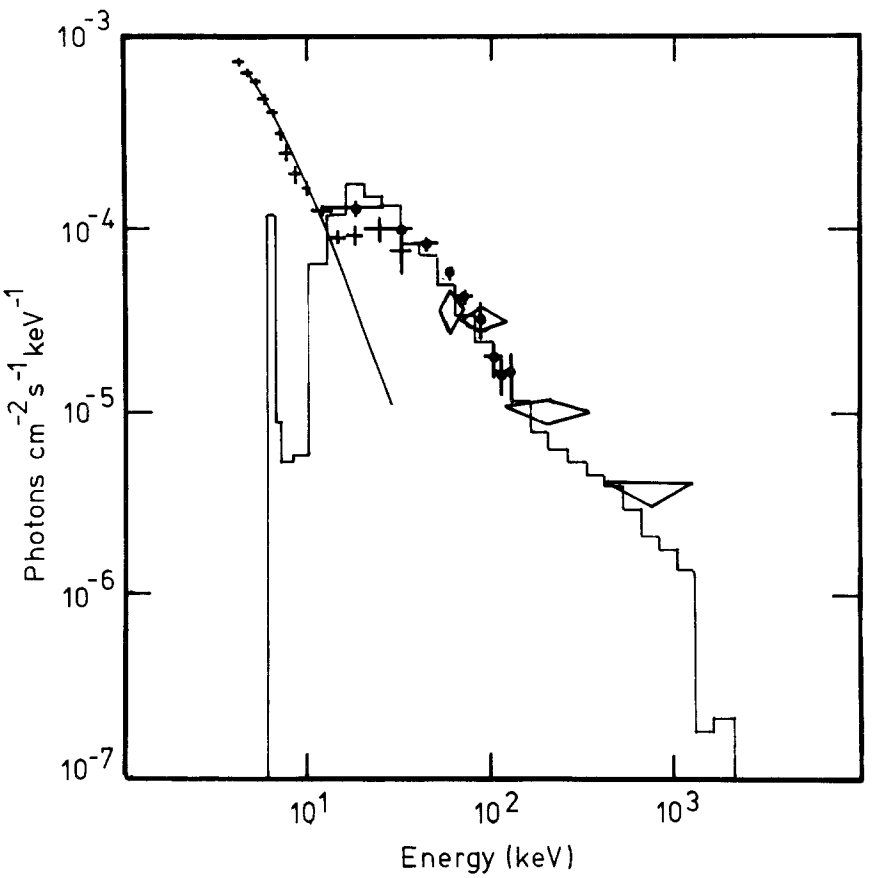

Fig. 7.3. The X-ray energy spectrum of SN 1987A in late August to early September obtained by combining the *Ginga* and the *Kvant* observations. The crosses are the data from *Ginga* in early September, the filled circles with error bars are the *Kvant* HEXE observations, and the diamonds represent the data from the Pulsar X-1 instrument. The histogram is the result of a model in which some of the ^{56}Co is mixed up into the hydrogen-rich layers (Itoh *et al.*, 1987b). The solid line is the theoretical spectrum expected if the soft X-ray emission is of thermal origin, caused by collision of the blast-wave with some residual circumstellar material (Masai *et al.*, 1987).

interaction of the blast wave with the pre-supernova wind (Chevalier and Fransson, 1987; Itoh *et al.*, 1987a, b). This said, it is somewhat curious that the rocket experiment by Aschenbach *et al.* (1987) found no evidence for flux in the 0.2–2.1 keV band on 24 August. If the soft X-rays are thermal, and are absorbed by the wind material, then this observation puts a useful lower limit on the pre-supernova mass loss, $\dot{M} \approx (2-5) \times 10^{-5} M_{\odot}\ \mathrm{yr}^{-1}$.

The flux above 30 keV is well-fitted by a Compton-degraded γ-ray spectrum. However, it does appear necessary to mix up at least some of the radioactive ^{56}Co to the outer, hydrogen-rich layers, or else to make the outer ejecta clumpy, to achieve a good fit with the shape and time-dependence of the X-ray spectrum. If the mantle is filled with fully opaque clumps with a constant total projected area, then the emergent X-rays will be 'gated' by the fraction of the total area covered by these blobs. The X-ray flux will then have the time dependence (Shull and Xu, 1987);

$$F_x(t) = F_0\{1 - (\alpha/t)^2\} \exp[-t/\tau_{\mathrm{Co}}]\,. \tag{7.6}$$

A relation of this form with $\alpha = 130 \pm 5$ days produces a remarkably good fit to the 10–30 keV flux observed by *Ginga* (see Figure 7.4), and provides powerful circumstantial evidence for a large-scale instability in the ejecta. Woosley *et al.* (1987b) has pointed out the mechanism whereby this could occur. Since the specific energy released in the radioactive decay processes is comparable to the energy density of the core material, the radioactivity can have important dynamic consequences. A low-density cobalt-rich

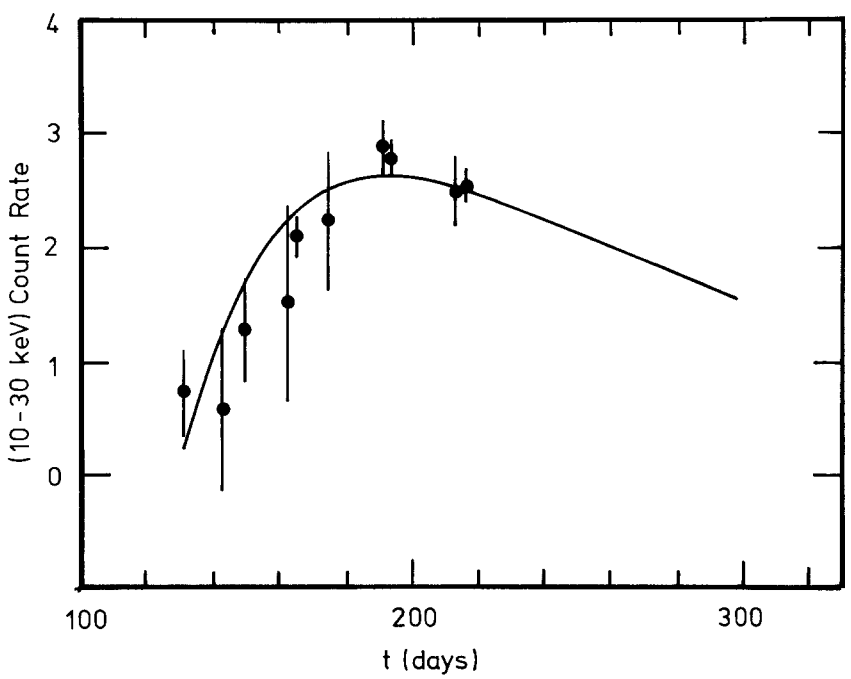

Fig. 7.4. The time variation of the X-ray flux observed by *Ginga* (Dotani *et al.*, 1987) compared with a simple model in which the obscuration is provided by dense cloudlets or blobs of ejecta (see text).

bubble will develop in the core of the fireball, pushing the material ahead into a dense shell. This shell has a thickness, L of about 10^{14} cm, and is accelerated at about 1–10 cm s^{-2}. It, therefore, will become Rayleigh–Taylor unstable on a time-scale of $(L/g)^{1/2} \approx 10^6$ to 10^7 s. This instability will probably allow us to see the neutron star rather earlier than spherically-symmetric models would lead us to suppose.

As the shell becomes increasingly transparent to the γ-rays, the bolometric luminosity (mainly emitted at optical and near IR wavelengths) is expected to decline more rapidly than the 113.7 day e-folding time-scale associated with the ^{56}Co decay. This deviation may have already commenced (at 300 days; see Figure 5.1), but the deviations should become more marked until by 700 days to luminosity will be about 65% of what would be expected by a simple extrapolation of the exponential portion (Nomoto and Shigeyama, 1987).

The conversion of the high-energy radiation to UV, optical and IR emission during the super-nebular phase is not simple. Fransson and Chevalier (1987) have made an initial examination of this problem by combining a Monte-Carlo treatment of the degradation of the γ-rays with a calculation of the ionization and temperature balance of the ejecta. This approach promises to provide a powerful tool for abundance and density diagnosis of the metal-rich ejecta, which in turn will provide the most direct means of examining the core of a massive star. The results show clearly the effects of composition. The Si–Ca zone is characterized by both Ca II] λ7300 Å and Ca II triplet emission at λ8400 Å (compare Figure 6.3), as well as Si I lines in the range $\lambda\lambda$1.6068–1.6455 μm, and [Si I] at λ1.0991 μm (compare Figures 6.7 and 6.8). The O–Mg Zone displays [O I] $\lambda\lambda$6300, 6363 Å, Mg I] λ4571 Å and Na I $\lambda\lambda$5890, 5896 Å emission (see Figure 6.3). As the expansion proceeds, the temperature remains of the order of a few thousand degrees. However, the heating per unit volume decreases faster than the cooling, and eventually an epoch is reached where the temperature falls catastrophically to around 300 K. The emission is then dominated by far-IR fine-structure line cooling, and by recombination lines.

At these epochs, dust formation becomes possible. Dwek (1987) has shown that its formation is critically dependent on the condensation temperature. If this is as high as 2000 K, then dust formation should have already begun, and the supernova would be very bright in the IR. Since this has not transpired, we must conclude that the condensation temperature is a good deal lower, in which case it is not likely to form.

Eventually, the shell will become transparent even to the escape of X-rays from the central pulsar. Before this phase is reached, however, the soft X-rays from an embedded pulsar may converted to UV emission (McCray *et al.*, 1987). This phase may have already started, since the UV emission is definately increasing. The UV flux should rise to about $2 \times 10^{37}[L_{\rm pulsar}/L_{\rm crab}]$ erg s^{-1}. If the central source is simply a hot cooling neutron star (Nomoto and Tsuruta, 1987), then the thermal emission falls very quickly initially due to plasmon-neutrino cooling near the surface. The dense core cools by Urca neutrino emission, but it takes at least 100 years for the cooling wave to reach the surface. The upshot of this is that the thermal X-ray emission is expected to fall very rapidly during the first two months or so, but the surface layers of the neutron state will

remain hot enough ($\log T \approx 6.4$–6.5 K), that thermal X-ray emission should be detectable for many years with planned X-ray missions.

8. Circumstellar and Interstellar Matter

8.1 Circumstellar matter

An enormous flurry of theoretical interest was created by the announcement in the IAU Telegrams, that speckle interferometric measurements had detected the presence of a source, apparently about three magnitudes fainter than SN 1987A at Hα, separated by some 60 milli-arc sec (mas) from the supernova itself (Karovska *et al.*, 1987; Nisenson *et al.*, 1987), corresponding to a linear distance of order 5×10^{16} cm. The presence of this source (at a distance of 74 mas) was apparently confirmed by another group (Matcher *et al.*, 1987; Meikle *et al.*, 1987). These observations spanned the time interval 25 March through to 14 April. If real, these observations define a source with extraordinary properties. It would have been just below mag 6, about 100 times brighter than any pre-existing star in the neighbourhood. The distance at which it was observed demands a speed of greater than about $0.5c$, if ejected from SN 1987A. The total energy emitted is at least 5×10^{44} ergs, if the emission is confined to the vicinity of Hα, however, the energy requirement becomes much higher if, as reported by Nisenson *et al.* (1987), the object was visible at other wavelengths. For these epochs, there is a definite non-detection in the infrared L-band (Perrier *et al.*, 1987).

Before considering the theoretical models devised to account for this source, let us critically examine the evidence for this source. Speckle interferometry is a notoriously difficult type of observation to make, since only a very small fraction of all photons contribute to the speckle power. Furthermore, it is very important that the photon counters used have a high dynamic range, do not display 'ringing' in their analogue signal, and do not otherwise introduce shifts in the photon addressing. It is not clear that these problems were completely eliminated in the data of Nisenson *et al.* (1987). The position angle of the source reported appears to be almost exactly along the scan direction of the detector. Furthermore, its separation, 59 mas, is almost identical with the position of the first maximum in the diffraction pattern (56 mas at Hα). The magnitude ratio, and somewhat smaller separation reported at shorter wavelengths also tend to suggest that the source was simply a portion of the first diffraction ring. As for the Meikle *et al.* data, the signal to noise ratio is simply insufficient to definitively detect a source three magnitudes fainter than the primary. Therefore, in the opinion of this reviewer, the reported detection of a second source should be treated with grave reserve.

Supposing that the 'mystery spot' was indeed real, what could possibly have given rise to it? The theories that have been put forward fall into two classes, direct ejection from the supernova event, and fluorescence from circumstellar material. Rees (1987) has suggested that the spot represents the escaping relativistic jet produced by puncturing of the plasma bubble about the newly formed pulsar. The emission is then produced by the synchrotron process in the vicinity of the bow shock or work surface. A somewhat

different picture is proposed by Piran and Nakamura (1987). This relies on the ejection of a polar-directed jet from the collapse of a rotating star. Nakamura and Sato (1981) found that their numerical simulations of core collapse showed a bounce which ejected as much as 0.007 $M_\odot$ along the poles at a velocity of about 0.6c. Although two blobs are produced in this picture, the luminosity ratio between the two is large because of relativistic effects, and only one is seen.

If SN 1987A had been a red supergiant, as seems necessary from the evolutionary considerations presented in Section 2, above, then we would expect to find some evidence of this phase of evolution in the form of circumstellar material. The possibility that a cloud of this material is fluorescently excited by the UV burst to produce the 'mystery spot' has been considered by Dopita *et al.* (1987a, b), Shaefer (1987), and Felten *et al.* (1988). We must remember that the wind from the red giant is shocked by the rejuvenated wind from the central star as it goes back to the blue. The ratio of the red giant wind density/blue supergiant wind density at all radii is

$$\rho_{rg}/\rho_{sg} = \dot{M}_{rg} V_{sg}/\dot{M}_{sg} V_{rg} \approx 900\,, \tag{8.1}$$

where $\dot{M}$ is the mass-loss rate, V is the wind velocity, and the subscripts refer to the red-giant and supergiant phases of evolution, respectively. The supergiant has a more energetic wind, $V_{sg} \approx 500$ km s^{-1}, and this drives a shock into the pre-existing red giant wind. The shock velocity, V_s, is given by

$$\rho_{rg} V_s^2 = \rho_{sg} V_{sg}^2\,, \tag{8.2}$$

hence, $V_s = 18$ km s^{-1}, approximately. If this shock is fully radiative (isothermal), then the post-shock density, ρ_f, is given in terms of the Mach number, M, of the shock by

$$\rho_f = \rho_{rg} M^2\,, \tag{8.3}$$

hence, assuming that the sound speed in the undisturbed medium is of order 1 km s^{-1}, the Mach number ~ 18. Therefore, using a red giant wind density of $n_{rg} = 3.1 \times 10^5$ cm^{-3}, appropriate to the mass-loss rate as a red giant, we find that $n_f = 1 \times 10^8$ cm^{-3} in the vicinity of the 'mystery spot'. At such high densities, the recombination time-scale is of order one day (Dopita *et al.*, 1987a–c), so that the blob would reprocess a portion of the energy of the UV flash rather promptly into a Balmer recombination spectrum. This model has energetic problems, since the angle subtended at the source by the blob is rather small and since the total energy of the UV flash is rather limited.

Mystery spot aside, the evidence for dense circumstellar material close to the star is incontrovertible. From far-UV spectra obtained with IUE since June, Kirshner (1987) has found evidence for narrow line emission, mainly in lines of nitrogen (see Figure 8.1). The intensity of these features have grown steadily, approximately linearly with time, as would be the case for a shell of material illuminated and ionized by the initial UV flash. The ionization state of this material is high, lines of N V, N IV, O IV, and Si IV being present, which is again consistent with photoionization by the UV flash, but at a lower density than that considered above.

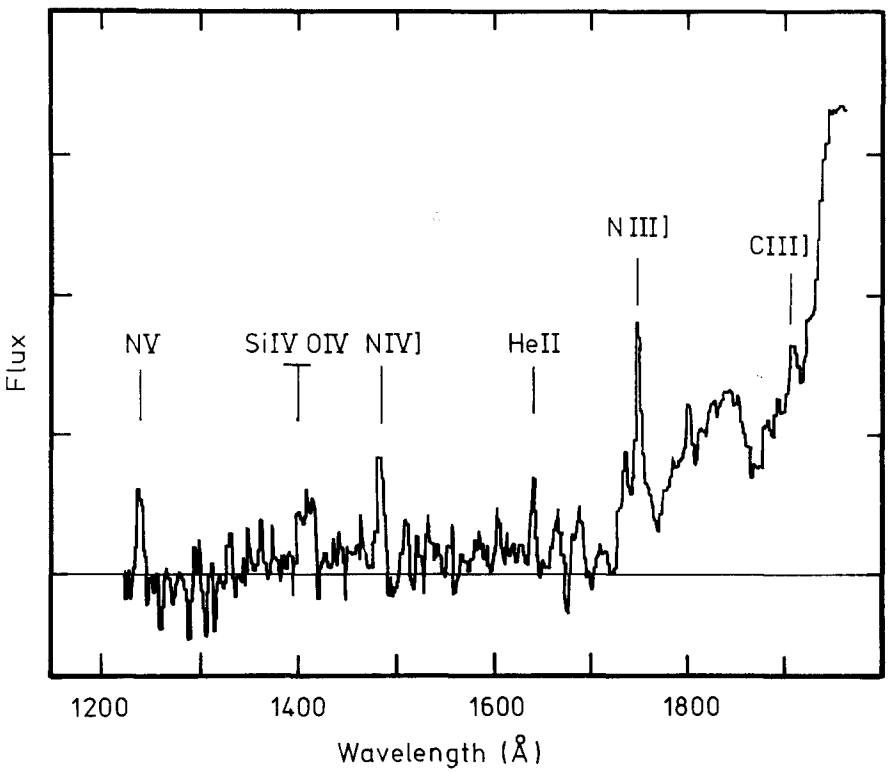

Fig. 8.1. The far-ultraviolet spectrum of SN 1987A observed in August with IUE, showing the narrow emission lines from photoionized circumstellar material. Data from several days have been averaged, and the spectrum in March (before the development of the narrow features) has been subtracted to remove the contributions of the companion stars (from Kirshner, 1987).

The circumstellar material might also become visible by its light echo of dust grains in the circumstellar environment. Schaefer (1987) has calculated that such an echos will be readily visible from even the interstellar material for many years to come. Perrier *et al.* (1987) have found evidence for reprocessing of optical radiation into IR radiation to produce an extended halo about SN 1987A visible by speckle interferometry in the IR L-band. This also became visible in mid-June, and shows a steady expansion since then. Rank *et al.* (1987) have argued that the IR flux distribution in the 5.3 to 12.6 μm band is also consistent with a dust-echo effect.

8.2. Interstellar absorption

For a brief moment in time, SN 1987A outshone all other sources in the LMC one thousandfold in the UV, thus giving a unique opportunity to examine a line-of-sight to LMC. Fortunately, the UV community proved equal to the challenge, and an excellent series of high dispersion spectra were obtained with IUE. The principal result of this work (Dupree *et al.*, 1987; de Boer *et al.*, 1987), was the discovery of lines covering an extremely wide range in ionization conditions. Table I is a summary list of lines detected.

TABLE I

UV Interstellar lines detected in SN 1987A (after Dupree *et al.*, 1987)

Ionic species	Wavelength (Å)	Ionic species	Wavelength (Å)
C I	1560.3, 1656.9	C II	1334.5
C IV	1548.2, 1550.8	O I	1302.2
Mg I	2025.8	Al II	1670.8
Al II	1854.7, 1862.8	Si II	1304.4, 1526.7, 1808.0
Si III	1206.5	Si IV	1393.7, 1402.8
S II	1250.6, 1253.8, 1259.5	Cr II	2055.6, 2065.5
Fe II	1608.5	Ni II	1741.6, 1751.9
Zn II	2025.5, 2062.0	Na I	2852.8, 2853.0
Mg I	2852.1	Mg II	2795.5, 2802.7
Mn II	2576.1, 2606.7	Fe II	2585.9, 2599.4
?	1259.6, 1717.1	?	1730.3, 1832.7

The Si IV and C IV lines are stronger than towards most LMC stars, with the notable exception of R136, the center of excitation of the 30 Doradus nebula. However, for N V, the observations establish an upper column density limit of $\log[N(\mathrm{N\,V})] \leq 14.5\ \mathrm{cm}^{-2}$, provided that the velocity dispersion is greater than 10 km s^{-1} (Fransson *et al.*, 1987). This figure, and the N V/C IV ratio puts useful limits on the temperature and the ionizating flux produced at the time of shock breakout (see also Section 4).

The ionizing flux, S, scales with the radius of the pre-supernova star, R, as

$$S = 10^{58}[R/3 \times 10^{13}\ \mathrm{cm}]^{-2}\ \mathrm{photons} \tag{8.4}$$

(Klein and Chevalier, 1978). The observations show that the ionizing flux was in fact less than about $10^{57}/n^2$ for a breakout temperature of about 5×10^5 K, which is consistent with the compact nature of the precursor.

A pronounced difference exists between the line-of-sight to R136 and the line-of-sight to SN 1987A. In the 30 Dor central region, the high excitation species, C IV, is blue-shifted with respect to the neutral gas by some 60 km s^{-1}. In the SN 1987A region, the high-excitation gas and the neutral gas both occur at about 275 km s^{-1}, heliocentric.

Unfortunately, the resolution provided by IUE was only equivalent to about 15–20 km s^{-1}, and this was insufficient to resolve the individual lines. Nevertheless, it is clear that absorption extends along all of the line of sight between us and the Supernova. At optical wavelengths, the interstellar absorption spectrum has been measured at resolutions of 10^5 (Andreani *et al.*, 1987; Vidal-Madjar *et al.*, 1987) to as high as 10^6 (Pettini and Gillingham, 1988). This work has demonstrated the existence of some 29 discrete clouds along the line-of-sight to the supernova. In Table II are summarized some of the key optical and UV absorption lines detected in these systems. Note in particular the detection of interstellar Li, detected for the first time in SN 1987A. In some of the UV clouds there is some ambiguity in assigning the identification, because the lines are broad, and the resolution is lower. Nevertheless, it is clear that at least some systems are detected only in the higher ionization species, and *vice versa*. There is a

TABLE II

Some absorption features in SN 1987A (data from Vidal-Madjar *et al.*, 1987; Pettini and Gillingham, 1987; de Boer *et al.*, 1987; and Magain 1987)

Cloud #	CaII	NaI	KI	CaI	LiI	CI	OI	MgI	SiII	AlII	AlIII	SiIV	CIV
1	−11												
2	9	9								3			
3		12				12		14	16		16	7	
4	16	18											19
5	23	24	22	24	(25)								
6	39									41		34	43
7	57						53		55				
8	65	64		65					65	67	69		
9	72	72						71	76				
10	81												
11	86												
12								114				105	116
13	123						125	126					
14											139	142	
15	162								160				160
16	166												
17	170						168	170					
18	175												
19	193												192
20	207											203	
21	216	216	213	216						215			
22	220	221					234			221	218		
23	250												
24	255	253	253										
25	266	266	266					261					
26	270	271	271		269								
27	280	281	280	280	280	275	275	277				277	
28	285									284			285
29	295		293	290									

consistent change in excitation conditions along the line-of-sight, based on the ratio of NaI/CaII.

The state of ionization of the gas associated with the LMC along the line-of-sight to SN 1987A is unusual, and significantly higher than that found in the line-of-sight to other stars in the LMC. In the optical, this is exemplified by the remarkable discovery of [FeX] absorption extending from 205 to 370 km s^{-1} (Pettini *et al.*, 1988; see Figure 8.3). If formed in collisional ionization equilibrium, this would require gas at $T \sim 10^6$ K. The equivalent width of this line, 16.4 mÅ, would imply a remarkably high FeX column density of 2.1×10^{17} cm^{-2} or an H^+ column density of 1.3×10^{22} cm^{-2} at LMC abundances. This is about five times higher than the HI column density in the same direction. There are two possibilities, either that the absorption is produced local to the star in a region which is denser than about 10^5 cm^{-3}, or else in an extended region about the star. The density implied by the local hypothesis is uncomfortably large, as the gas would cool and recombine very quickly. The most likely explanation for this is

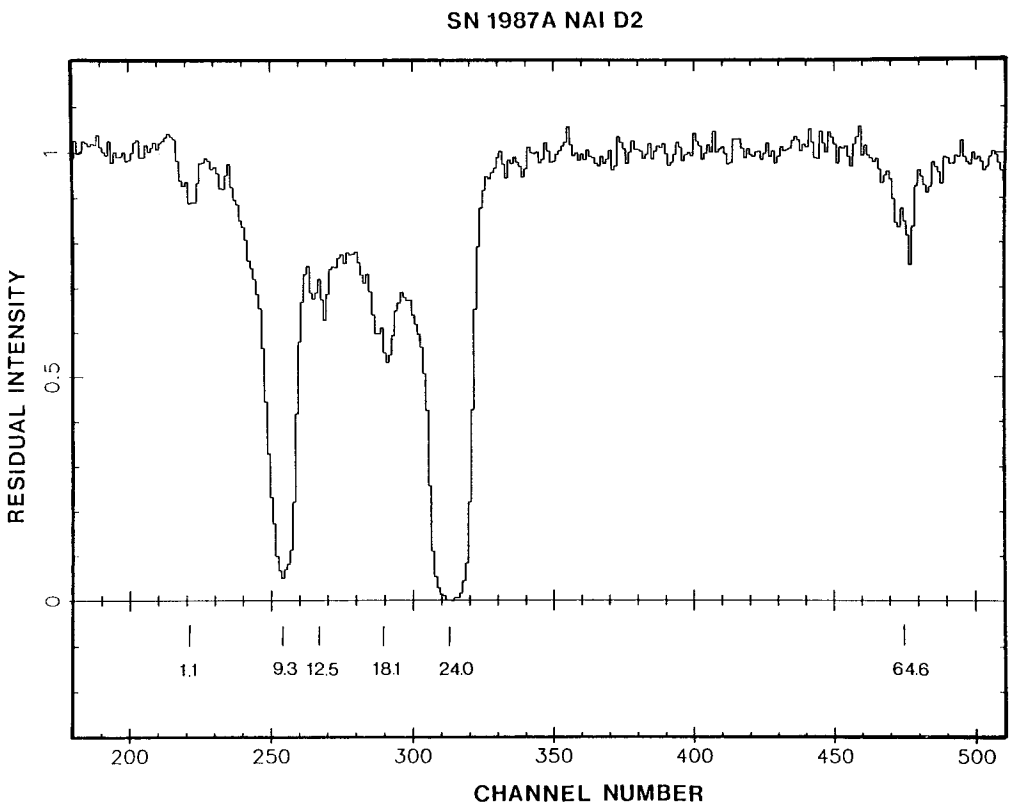

Fig. 8.2. The detection of hyperfine splitting in Na absorbing clouds along the line-of-sight to SN 1987A (after Pettini *et al.*, 1988). The features at 1.1, 12.5, 18.1, and 64.6 km s^{-1} clearly display this splitting.

that the supernova exploded inside a pre-existing bubble of hot gas generated by previous supernova events in the same region. Such regions have been identified elsewhere in the LMC (Dopita, 1985) and indeed, the Sun itself may lie in a similar, if somewhat less energetic region (Tanaka and Bleeker, 1977; Jacobsen and Kahn, 1986).

9. What Is There Left to Learn

The explosion of SN 1987A has provided us with a new insight into Type II events, showing for the first time the intimate relationship between the metallicity of the galaxy, the structure of the precursor star, and the nature of the display. It has established the existence of a new class of very dim Type II events, resulting from the explosion of a compact precursor (although presently this class has only a membership of one!). The fact that SN 1987A had a perfectly unremarkable precursor in the context of the population of bright stars in the LMC must imply that such events are by no means rare in systems of low metallicity, and, therefore, that the Type II supernova rates estimated for such systems (e.g., Tammann, 1982) must be grossly in error. It would be very important to establish to what metallicity this remains true, since this offers some chance

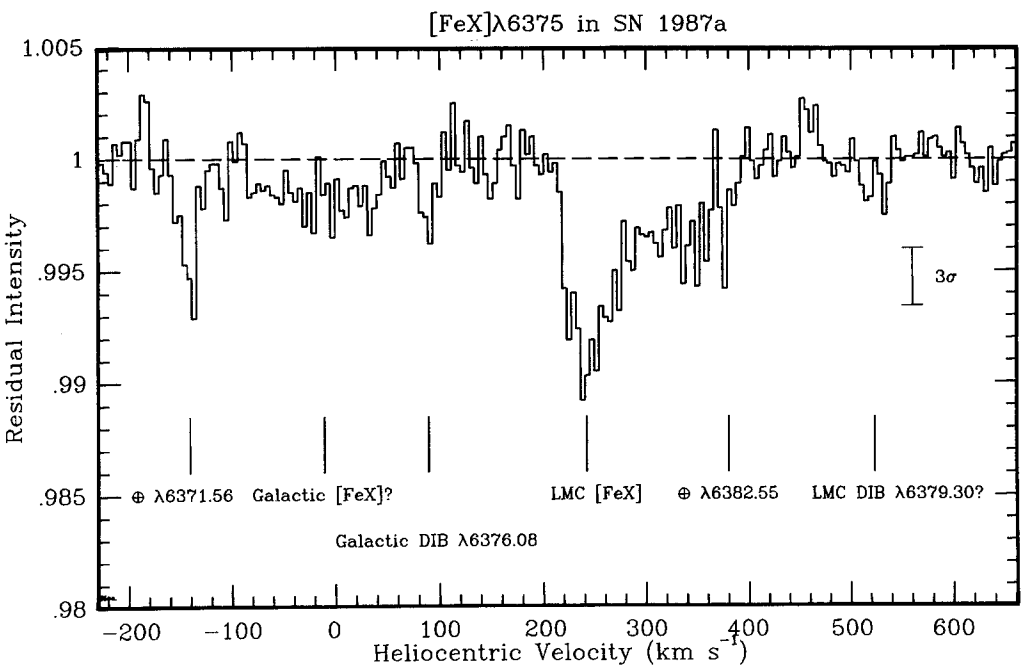

Fig. 8.3. The detection of interstellar [Fe X] in the line-of-sight to SN 1987A (from Pettini *et al.*, 1988). Note that the central depth of this feature is only 1%, and that the absorption structure does not correspond particularly to any of the clouds of Table II.

of reconciling the estimated birthrate of neutron stars with the rate of supernova explosions in our Galaxy.

The interpretation of the structure of the upper H–R diagram (Figure 2.2) is complicated by the fact that it is populated both by stars moving redwards, and by more evolved stars returning to the blue. Clearly, a result of the renewed interest generated by the supernova will be some improvement in stellar evolution codes. Observationally, we could expect to distinguish the various ages of stars spectroscopically, if other stars in their late evolutionary phases show the same enhancements of CN-processed elements and *s*-process elements that apparently characterized Sk – 69°202. SN 1987A has established that stars with helium cores as small as 6 $M_\odot$ are capable of returning to the blue. This will help to explain the distribution of stars in the upper H–R diagram, which has been a long-standing problem. The mass on the ZAMS must have only have been about 15 $M_\odot$, so stars which give 'classical' Type II displays must be less massive than this. However, the lower mass for Type II events is in the range 8–10 $M_\odot$, so classical Type II events can only occur over a very narrow mass range in the LMC.

The theoretical scenario for the core collapse and the formation of a neutron star appears to have been very well supported by the observations of the neutrino burst, although the exact relationship between the core collapse, and the subsequent explosion remains unclear. The prospects for neutrino astronomy are good, and it is to be hoped that much larger water Čerenkov observatories are built to investigate the physics of core

collapse in more detail, and to probe for supernova explosions throughout the local group of galaxies. To give data of comparable quality to SN 1987A in M33 or M31 would require a detector about 30 000–100 000 tons.

The radio burst observed in the first few weeks proved the existence of a wind, but, if our picture of the precursor star is correct, it was just a firecracker compared with the outburst to be expected when the blast-wave runs into the circumstellar material. The Australia Telescope will be ideally suited to study the evolution of this event over the next twenty years or so, and the development of the synchrotron-powered nebulosity around the central pulsar. Unfortunately, it is likely to be so bright as to seriously compromise observations of other sources in the LMC.

The explosion of SN 1987A has emphasized the need for improved atmospheric models of Type II events. These need to take into account non-LTE effects, line blocking and relativistic effects in order to describe both line formation and the continuum distribution. Both of these are needed if ever the Type II are to be used to determine the Hubble Constant in their own right. The possibility of following the detailed spectral evolution to very late phases is particularly exciting. We expect the nebular phase to develop to the point where catastrophic cooling of the metal-rich ejecta occurs, when the energy input from radioactive decay becomes insufficient. This may be an epoch of dust formation. In this late phase we can also expect to see the emergence of the neutron star which we confidently predict to be present. Many groups are already geared up to look for pulsed optical emission from this object.

The X-ray spectroscopic results are also in good agreement with the theoretical expectations. As the fireball becomes increasingly optically thin, we can expect the rate of decline of the bolometric luminosity to accelerate. There are already some suggestions (at 300 days) that this has started to occur in the V magnitude. There appears to be clear evidence for the Rayleigh–Taylor unstable break-up of the inner ejecta as a result of the development of the 'Ni-bubble' in the center. Such an instability may be enhanced by the thermal instability expected in the metal-rich as this cools. Such processes are certainly the cause of the oxygen-rich knots seen in young supernova remnants when these plow through the inwardly-propagating reverse shock.

References

Aglietta, M., Badino, G., Blogna, G. F., Castagnoli, C., Castellina, A., Fulgione, W., Galeotti, P., Saavedra, O., Trinchero, G., Vernetto, S., Dadykin, V. L., Kortchaguin, V. B., Malguin, A. S., Ryassny, V. G., Ryazhskaya, O. G., Talochkin, P. V., Zatespin, G. T., and Yakushev, V. F.: 1987, *Europhys. Letters* **3**, 1315.

Aitken, D., Smith, C. H., James, S. D., Roche, P. F., Hyland, A. R., and McGregor, P.: 1987, *Monthly Notices Roy. Astron. Soc.* (in press).

Andreani, P., Ferlet, R., and Vidal-Madjar, A.: 1987, preprint.

Arnett, W. D.: 1980, *Astrophys. J.* **237**, 541.

Arnett, W. D.: 1987a, *Astrophys. J.* **319**, 136.

Arnett, W. D.: 1987b, *Astrophys. J.*(in press).

Aschenbach, B., Briel, U. G., Pfeffermann, E., Bräuninger, H., Hippmann, H., and Trümper, J.: 1987, *Nature* **330**, 232.

Ashoka, B. N., Anupama, G. C., Prabhu, T. P., Giriidhar, S., Ghash, K. K., Jain, S. K., Pati, A. K., and Kameswara Rao, N.: 1987, *J. Astrophys. Astron.* **8**, 195.
Bahcall, J. N., Dar, A., and Piran, T.: 1987a, *Nature* **326**, 135.
Bahcall, J. N., Piran, T., Press, W. H., and Spergel, D. N.: 1987b, *Nature* **327**, 682.
Barkat, Z. and Wheeler, J. C.: 1988, *Astrophys. J.* (in press).
Bartunov, O. S. and Tsvetkov, D. Yu.: 1986, *Astrophys. Space Sci.* **122**, 343.
Bethe, H., Yahil, A., and Brown, G. E.: 1982, *Astrophys. J.* **262**, L7.
Bionta, R. M., Blewitt, G., Bratton, C. B., Casper, D., Ciocio, A., Claus, R., Cortez, B., Crouch, M., Dye, S. T., Errede, S., Foster, G. W., Gajewski, W., Ganezer, K. S., Goldhaber, M., Haines, T. J., Jones, T. W., Kielczewska, D., Kropp, W. R., Learned, J. G., LoSecco, J. M., Mattews, J., Miller, R., Mudan, M. S., Park, H. S., Price, L. R., Reines, F., Shultz, J., Seidel, S., Shumard, E., Sinclair, D., Sobel, H. W., Stone, J. L., Sulak, L. R., Svboda, R., Thornton, G., van der Velde, J. C., and Wuest, C.: 1987, *Phys. Rev. Letters* **58**, 1494.
Blanco, V. M., Gregory, B., Hamuy, M., Heathcote, S. R., Phillips, M. M., Suntzeff, N. B., Terndrup, D. M., Walker, A. R., Williams, R. E., Pastoriza, M. G., and Storchi-Bergmann, T.: 1987, *Astrophys. J.* **320**, 589.
Branch, D.: 1987a, *Astrophys. J.* **320**, L23.
Branch, D.: 1987b, *Astrophys. J.* **320**, L121.
Brown, G. E., Bethe, H. A., and Baym, G.: 1981, *Nucl. Phys.* **A375**, 481.
Bruenn, S. W.: 1987, *Phys. Rev. Letters* **59**, 938.
Brunet, J. P.: 1975, *Astron. Astrophys.* **43**, 345.
Burrows, A.: 1984, *Astrophys. J.* **283**, 848.
Burrows, A. and Lattimer, J. M.: 1987, *Astrophys. J.* **318**, L63.
Carney, B. W.: 1980, *Publ. Astron. Soc. Pacific* **92**, 56.
Cassatella, A., Fransson, C., van Santvoort, J., Gry, C., Talavera, A., Wamsteker, W., and Panagia, N.: 1987a, *Astron. Astrophys.* **177**, L29.
Cassatella, A., Wamsteker, W., Sanz, L., and Gry, C.: 1987b, *IAU Circ.*, No. 4330.
Catchpole, R. M., Menzies, J. W., Monk, A. S., Wargau, W. F., Pollacco, D., Carter, B. S., Whitelock, P. A., Marang, F., Laney, C. D., Balona, L. A., Feast, M. W., Lloyd Evans, T. H. H., Sekiguchi, K., Laing, J. D., Kilkenny, D. M., Spencer Jones, J., Roberts, G., Cousins, A. W. J., van Vuuren, G., and Winkler, H.: 1987, *Monthly Notices Roy. Astron. Soc.* **229**, 15 p.
Chevalier, R. E. and Fransson, C.: 1987, *Nature* **328**, 44.
Chugaj, N.: 1987, Astronomical Preprints, Soviet Academy of Sciences, No. 1494.
Cristiani, S., Babel, J., Barwig, H., Clausen, J. V., Gouiffes, C., Günter, T., Helt, B. E., Heynderickx, D., Loyola, P., Magnusson, P., Monderen, P., Rabattu, X., Sauvageout, J. L., Schoembs, R., Schwarz, H., and Steenman, F.: 1987, *Astron. Astrophys* **177**, L5.
Cropper, M., Bailey, J., McCowage, J., Cannon, R. D., Couch, W. J., Walsh, J. R., Straede, J. O., and Freeman, F.: 1987, *Monthly Notices Roy. Astron. Soc.* (in press).
Danziger, I. J., Fosbury, R. A. E., Alloin, D., Cristiani, S., Dachs, J., Gouiffes, C., Jarvis, B., and Sahu, K. C.: 1987, *Astron. Astrophys.* **177**, L13.
De Boer, K. S., Gewing, M., Richtler, T., Wamsteker, W., Gry, C., and Panagia, N.: 1987, *Astron. Astrophys.* **177**, L37.
D'Odorico, S., Molaro, P., Pettini, M., Stathakis, R., and Vladilo, G.: 1987, in *Proceedings of ESO Workshop 'SN 1987A'*, ESO, Garching.
Dopita, M. A.: 1985, in W. Boland and H. van Woerden (eds.), *Birth and Evolution of Massive Stars and Stellar Groups*, D. Reidel Publ. Co., Dordrecht, Holland, p. 269.
Dopita, M. A.: 1986, 'Star-Forming Regions', in M. Peimbert and J. Jugaku (eds.), *IAU Symp.* **115**, 501.
Dopita, M. A.: 1987a, *Nature* (in press).
Dopita, M. A.: 1987b, 'Atmospheric Diagnostics of Stellar Evolution', in K. Nomoto (ed.), *IAU Colloq.* **108**.
Dopita, M. A., Achilleos, N., Dawe, J. A., Flynn, C., and Meatheringham, S. J.: 1987a, *Proc. Astron. Soc. Australia* 7 (in press).
Dopita, M. A., Dawe, J. A., Achilleos, N., Brissenden, R. J. V., Flynn, C., Meatheringham, S. J., Rawlings, S., Tuohy, I. R., McNaught, R. D., Coates, D. W., Hancy, S., Thompson, K., and Shobbrook, R. R.: 1987b, *Astron. J.* (in press).
Dopita, M. A., Meatheringham, S. J., Nulsen, P., and Wood, P.: 1987c, *Astrophys. J.* **322**, L85.
Dotani, T., Hayashida, K., Inoue, H., Itoh, M., Koyama, K., Makino, F., Mitsuda, K., Murakami, T., Oda, M., Ogawara, Y., Takano, S., Tanaka, Y., Yoshida, A., Makishima, K., Ohashi, T., Kawai, N., Matsuoka,

M., Hoshi, R., Hayakawa, S., Kii, T., Kunieda, H., Nagase, F., Tawara, Y., Hatskade, I., Kitamota, S., Miyamoto, S., Tsunemi, H., Yamashita, K., Nakagawa, M., Yamauchi, M., Turner, M. J. L., Pounds, K. A., Thomas, H. D., Stewart, G. C., Cruise, A. M., Patchett, B. E., and Reading, D. H.: 1987, *Nature* **330**, 230.

Dupree, A. K., Kirshner, R. P., Nassiopoulos, G. E., Raymond, J. C., and Sonneborn, G.: 1987, *Astrophys. J.* **320**, 602.

Dwek, E.: 1987, *Astrophys. J.* Letters (in press).

Edwards, P. J.: 1987, *Proc. Astron. Soc. Australia* **7** (in press).

Falk, S. W. and Arnett, W. D.: 1977, *Astrophys. J. Suppl.* **33**, 515.

Feast, M. W.: 1984, *South African Observatory Circ.*, No. 397.

Feast, M. W.: 1986, in B. F. Madore and R. B. Tully (eds.), *Galaxy Distances and Deviations from Universal Expansion*, D. Reidel Publ. Co., Dordrecht, Holland, p. 7.

Felten, J. E., Dwek, E., and Viegas-Aldrovandi, S. M.: 1988, *Nature* (in press).

Filippenko, A. V. and Sargent, W. L. W.: 1985, *Nature* **316**, 407.

Filippenko, A. V. and Sargent, W. L. W.: 1986, *Astron. J.* **91**, 691.

Fitzpatrick, E. L.: 1985, *Astrophys. J.* **299**, 219.

Fransson, C. and Chevalier, R. A.: 1987, *Astrophys. J.* **322**, L15.

Fransson, C., Grewing, M., Cassatella, A., Panagia, N., and Wamsteker, W.: 1987, *Astron. Astrophys.* **177**, L33.

Fukugita, M. and Nakamura, T.: 1987, *Phys. Rev. Letters* (in press).

Gehrels, N., MacCullum, C. J., and Leventhal, M.: 1987, *Astrophys. J.* **320**, L19.

Gilmozzi, R., Cassatella, A., Clavel, J., Fransson, C., Gonzalez, R., Gry, C., Panagia, N., Talavera, A., and Wamsteker, W.: 1987, *Nature* **328**, 318.

Grassberg, E. K., Imshennik, V. S., Nadyozhin, D. K., and Utrobin, V. P.: 1987, ITEP Preprint No. 57.

Grebenev, S. A. and Sunyaev, R. A.: 1987, *Soviet Astron. Letters* **13**, 945.

Hamuy, M., Suntzeff, N. B., Gonzalez, R., and Martin, G.: 1987, *Astrophys. J.* (in press).

Hanuschik, R. W. and Dachs, J.: 1987a, *Astron. Astrophys.* **182**, L29.

Hanuschik, R. W. and Dachs, J.: 1987b, in J. Danziger (ed.), *Proceedings of ESO Workshop on SN 1987A*, ESO, Garching.

Harwit, M., Biermann, P. L., Meyer, H., and Wasserman, I. M.: 1987, *Nature* **328**, 503.

Haubold, H. J., Kaempfer, B., Senatorov, A. V., and Voskresenski, D. N.: 1987, *Astron. Astrophys.* (in press).

Hershkowitz, S., Linder, E., and Wagoner, R. V.: 1986, *Astrophys. J.* **301**, 220.

Hillebrandt, W.: 1985; in I. J. Danziger, F. Matteucci, and K. Kjär (eds.), *Production and Distribution of C, N, O Elements*, Proc. of ESO Workshop, ESO, Garching.

Hillebrandt, W., Höflich, P., Kafka, P., and Müller, E.: 1987a, *Astron. Astrophys.* **180**, L20.

Hillebrandt, W., Höflich, P., Kafka, P., Müller, E., Schmidt, H. U., and Truran, J. W.: 1987b, *Astron. Astrophys.* **177**, L41.

Hillebrandt, W., Höflich, P., Truran, J. W., and Weiss, A.: 1987c, *Nature* **327**, 597.

Hirata, K., Kajita, T., Koshiba, M., Nakahata, M., Oyama, Y., Sato, N., Suzuki, A., Takita, M., Totsuka, Y., Kifune, T., Suda, T., Takahashi, K., Tanimori, T., Miyano, K., Yamada, M., Beier, T., Kim, S. B., Mann, A. K., Newcomer, F. M., Van Berg, R., and Zhang, W.: 1987, *Phys. Rev. Letters* **58**, 1490.

Höfflich, P.: 1987, in *Proc. of the 4th Workshop on Nuclear Astrophysics*, Ringberg Castle.

Höfflich, P., Wehrse, R., and Shaviv, G.: 1986, *Astron. Astrophys.* **163**, 105.

Humphreys, R. M. and McElroy, D. B.: 1984, *Astrophys. J.* **284**, 565.

Imshennik, V. S. and Nadyozhin, D. K.: 1964, *Astron. Zh.* **41**, 829.

Isserstedt, J.: 1975, *Astron. Astrophys.* **41**, 175.

Itoh, H., Hayakawa, S., Masai, K., and Nomoto, K.: 1987, *Publ. Astron. Soc. Japan* **39**, 529.

Itoh, H., Kumagai, S., Shigeyama, T., Nomoto, K., and Nishimura, J.: 1987, *Nature* **330**, 233.

Jakobsen, P. and Kahn, S. M.: 1986, *Astrophys. J.* **309**, 682.

Jeffery, D. J.: 1987, *Nature* **329**, 419.

Karosvska, M., Nisenson, P., Noyes, R., and Papaliolios, C.: 1987, *IAU Circ.*, No. 4382.

Kirshner, R. P. and Kwan, J.: 1974, *Astrophys. J.* **193**, 27.

Kirshner, R. P. and Kwan, J.: 1974, *Astrophys. J.* **193**, 27.

Kirshner, R. P., Oke, J. B., Penston, M. V., and Searle, L.: 1973, *Astrophys. J.* **185**, 303.

Kirshner, R. P.: 1987, 'Atmospheric Diagnostics of Stellar Evolution', in K. Nomoto (ed.), *IAU Colloq.* **108**.

Kirshner, R. P., Sonneborn, G., Crenshaw, D. M., and Nassiopoulos, G. E.: 1987, *Astrophys. J.* **320**, 602.

Klein, R. I. and Chevalier, R. A.: 1978, *Astrophys. J.* **223**, L109.
Krauss, L. M.: 1987, *Nature* **329**, 689.
Kumagai, S., Itoh, M., Shigeyama, T., Nomoto, K., and Nishimura, J.: 1987, in M. Kafatos (ed.), *Proceedings of the George Mason Workshop on 'Supernova 1987A in the Large Magellanic Cloud'*, Cambridge University Press, Cambridge (in press).
Lucy, L. B.: 1987, *Astron. Astrophys.* **182**, L31.
Maeder, A.: 1987, 'Atmospheric Diagnostics of Stellar Evolution', in K. Nomoto (ed.), *IAU Colloq.* **108** (in press).
Magain, P.: 1987, *Nature* **329**, 606.
McCall, M. L.: 1984, *Monthly Notices Roy. Astron. Soc.* **210**, 829.
McCray, R., Shull, J. M., and Sutherland, P.: 1987, *Astrophys. J.* **317**, L73.
McGregor, P. J., Hyland, A. R., Ashley, M. C. B., and Straw, S.: 1988 (in preparation).
McNamara, D. H. and Feltz, K. A., Jr.: 1980, *Publ. Astron. Soc. Pacific* **92**, 587.
Marcher, S. J., Meikle, W. P. S., and Morgan, B. L.: 1987, *IAU Circ.*, No. 4391.
Masai, K., Hayakawa, S., Itoh, H., and Nomoto, K.: 1987, *Nature* **330**, 235.
Matcher, S. J., Meikle, W. R. S., and Morgan, B. L.: 1987, *IAU Circ.*, No. 4369.
Meikle, W. P. S., Matcher, S. J., and Morgan, B. L.: 1987, *Nature* **329**, 608.
Menzies, J. W., Catchpole, R. M., van Vuuren, G., Winkler, H., Laney, C. D., Whitelock, P. A., Cousins, A. W. J., Carter, B. S., Marang, F., Lloyd Evans, T. H. H., Roberts, G., Kilkenny, D., Spencer Jones, J., Sekiguchi, K., Fairall, A. P., and Wolstencroft, R.: 1987, *Monthly Notices Roy. Astron. Soc.* **227**, 39 p.
Miyaji, S. and Saio, H.: 1987, *IAU Colloquium #108*; 'Atmospheric Diagnostics of Stellar Evolution', in K. Nomoto (ed.), *IAU Colloq.* **108** (in press).
Nakamura, T. and Sato, H.: 1981, *Prog. Theor. Phys.* **66**, 2038.
Nisenson, P., Papiolios, C., Karovska, M., and Noyes, R.: 1987, *Astrophys. J.* **320**, L15.
Nomoto, K. and Shigeyama, T.: 1987, in M. Kafatos (ed.), *Proceedings of the George Mason Workshop on 'Supernova 1987A in the Large Magellanic Coud'*, Cambridge University Press, Cambridge (in press).
Nomoto, K., Shigeyama, T., and Hashimoto, T.: 1987, in J. Danziger (ed.), *Proceedings of ESO Workshop on 'SN 1987A'*, ESO, Garching.
Nomoto, K. and Tsuruta, S.: 1987, in M. Kafatos (ed.), *Proceedings of the George Mason Workshop on 'Supernova 1987A in the Large Magellanic Cloud'*, Cambridge University Press, Cambridge (in press).
Ostriker, J. P.: 1987, *Nature* **327**, 287.
Panagia, N.: 1985, in Norbert Bartel (ed.), 'Supernovae as Distance Indicators', *Lecture Notes in Physics*, Vol. 224, Springer-Verlag, Berlin, p. 14.
Panagia, N., Gilmozzi, R., Clavel, J., Barylak, M., Gonzalez Riesta, R., Lloyd, C., Sanz Fernandez de Cordoba, L., and Wamsteker, W.: 1987, *Astron. Astrophys.* **177**, L25.
Perrier, C., Chalabaev, A. A., Mariotti, J. M., and Bouchet, P.: 1987, in J. Danziger (ed.), *Proceedings of ESO Workshop on 'SN 1987A'*, ESO, Garching.
Pettini, M. and Gillingham, P. R.: 1988 (in preparation).
Pettini, M., Stathakis, R., D'Odorico, S., Molaro, P., and Vladilo, G.: 1988, *Astrophys. J.* (in press).
Pinto, P. and Woosley, S. E.: 1987, preprint.
Piran, T. and Nakamura, T.: 1987, *Nature* **330**, 28.
Rank, D. M., Bregman, J., Witteborn, F. C., Cohen, M., Lynch, D. K., and Russell, R. W.: 1987, *Astrophys. J.* (in press).
Rees, M. J.: 1987, *Nature* **328**, 207.
Rousseau, J., Martin, N., Prévot, L., Rebeirot, A. R., and Brunet, J. P.: 1978, *Astron. Astrophys. Suppl. Ser.* **31**, 243.
Russell, S. C., Bessell, M. S., and Dopita, M. A.: 1987, *NATO Advanced Study Institute on 'Star Formation'*, Calgary, Canada.
Ryder, S.: 1987, internal report, Univ. of Canterbury, Christchurch, New Zealand.
Sato, K. and Suzuki, H.: 1987, *Phys. Rev. Letters* **58**, 2722.
Schaefer, B. E.: 1987, *Astrophys. J.* **323**, L47.
Schaeffer, R., Cassé, M., and Cahen, S.: 1987a, *Astrophys. J.* **316**, L31.
Schaeffer, R., Cassé, M., Mochkovitch, R., and Cahen, S., 1987b, *Astron. Astrophys.* **184**, L1.
Schaeffer, R., Declais, Y., and Jullian, S.: 1987c, *Nature* **330**, 142.
Schwarz, H. E. and Mundt, R.: 1987, *Astron. Astrophys.* **177**, L4.
Shara, M., McLean, B., and Sanduleak, N.: 1987, *IAU Circ.*, No. 4318.

Shklovski, I. S.: 1984, *Pis'ma Astron. Zh.* **10**, 723.
Shklovski, I. S.: 1985, in *Stars: Their Birth, Life and Death*, 3rd ed., Nauka, Moscow.
Shull, J. M. and Xu, Y.: 1987, in M. Kafatos (ed.), *Proc. George Mason Conference on SN 1987A*, Cambridge University Press, Cambridge.
Shigeyama, T., Nomoto, K., Hashimoto, M., and Sugimoto, D.: 1987, *Nature* **328**, 320.
Sneden, C.: 1985, in I. J. Danziger, F. Matteuci, and K. Kjär (eds.), *Proceedings of ESO Workshop on 'Production and Distribution of C, N, O Elements'*, ESO, Garching, p. 1.
Sonneborn, G. and Kirshner, R. P.: 1987, *IAU Circ.*, No. 4333.
Sonneborn, G. Altner, B., and Kirshner, R. P.: 1987, *Astrophys. J.* (in press).
Spies, W., Hauschildt, P., Wehrse, R., Baschek, B., and Shaviv, G.: 1987a, *Proc. 4th Workshop on 'Nuclear Astrophysics'*, Ringberg Castle, W. Germany.
Spies, W., Hauschildt, P., Wehrse, R., and Shaviv, G.: 1987b, *Astrophys. J.* (in press).
Storey, M. C. and Manchester, R. N.: 1987, *Nature* **329**, 421.
Sunyaev, R., Kaniovskiy, A., Efremov, V., Gilfanov, M., Churazov, E., Grebenev, S., Kuznetsov, A., Melioranskiy, A., Yamburenko, N., Yumin, S., Stepanov, D., Chulkov, I., Pappe, N., Boyarskiy, M., Gavrilova, E., Loznikov, V., Prudkogiyad, A., Rodin, V., Reppin, C., Pietsch, W., Engelhauser, J., Trimper, J., Vogen, W., Kendziorra, E., Bezler, M., Staubert, R., Brinkman, A. C., Heise, J., Mels, W. A., Jager, R., Skinner, G. K., Al-Emam, O., Patterson, T. G., and Willmore, A. P.: 1987, *Nature* **330**, 227.
Suzuki, H. and Sato, K.: 1987, *Publ. Astron. Soc. Japan* **39**, 521.
Tammann, G. A.: 1982, in M. J. Rees and R. J. Stoneham (eds.), *Supernovae: A Survey of Current Research*, D. Reidel Publ. Co., Dordrecht, Holland.
Tanaka, Y. and Bleeker, J. A. M.: 1977, *Space Sci. Rev.* **20**, 815.
Turtle, A. J., Campbell-Wilson, D., Bunton, J. D., Jauncey, D. L., Kesteven, M. J., Manchester, R. N., Norris, R. P., Storey, M. C., and Reynolds, J. F.: 1987, *Nature* **327**, 38.
Vidal-Madjar, A., Andreani, P., Cristiani, S., Ferlet, R., Lanz, T., and Vladilo, G.: 1987, *Astron. Astrophys.* **177**, L17.
Vladilo, G., Crivellari, L., Molaro, P., and Beckman, J. E.: 1987, *Astron. Astrophys.* **182**, L59.
Vladilo, G.: 1987, *The Messanger (E.S.O.)* **47**, 29.
Wagoner, R.: 1987, 'Atmospheric Diagnostics of Stellar Evolution', in K. Nomoto (ed.), *IAU Colloq.* **108** (in press).
Walborn, N. R., Lasker, B. M., Laidler, V. G., and Chu, Y.-H.: 1987, *Astrophys. J.* **321**, L41.
Walborn, N. R.: 1987, 'Atmospheric Diagnostics of Stellar Evolution', in K. Nomoto (ed.), *IAU Colloq.* **108** (in press).
Waldron, W. L.: 1985, in A. B. Underhill and A. G. Michelitsianos (eds.), *The Origin of Nonradiative Heating/Momentum in Hot Stars*, NASA Conf. Publ. CP-2358, p. 95.
Wamsteker, W., Panagia, N., Barylak, M., Cassatella, A., Clavel, J., Gilmozzi, R., Gry, C., Lloyd, C., van Santvvort, J., and Talavera, A.: 1987, *Astron. Astrophys.* **177**, L21.
Wampler, E. J., Truran, J. W., Lucy, L. B., Höflich, P., and Hillebandt, W.: 1987, *Astron. Astrophys.* **182**, L51.
Weaver, T. A., Axelrod, T. S., and Woosley, S. E.: 1980, in J. C. Wheeler (ed.), *Proceedings of Texas Workshop on 'Type I Supernovae'*, University of Texas, Austin, p. 113.
Weiler, K. W.: 1985, in Norbert Bartel (ed.), 'Supernovae as Distance Indicators', *Lecture Notes in Physics* **224**, Springer-Verlag, Berlin, p. 65.
West, R. M., Lauberts, A., Jørgensen, H. E., and Schuster, H.-E.: 1987, *Astron. Astrophys.* **177**, L1.
Wheeler, J. C., Harkness, R. P., and Barkat, Z.: 1987a, 'Atmospheric Diagnostics of Stellar Evolution', in K. Nomoto (ed.), *IAU Colloq.* **108** (in press).
Wheeler, J. C., Harkness, R. P., and Barkat, Z.: 1987b, in M. Kafatos (ed.), *Proceedings of the George Mason Workshop on 'Supernova 1987A in the Large Magellanic Cloud'*, Cambridge University Press, Cambridge.
White, G. L. and Malin, D. F.: 1987a, *IAU Circ.*, No. 4330.
White, G. L. and Malin, D. F.: 1987b, *Nature* **327**, 36.
Wilson, J. R., Mayle, R., Woosley, S. E., and Weaver, T. A.: 1986, *Ann. N.Y. Acad. Sci.* **470**, 267.
Williams, R. E.: 1987, *Astrophys. J.* **320**, L117.
Wood, P. R. and Faulkner, D. J.: 1987, *Proc. Astron. Soc. Australia* **7**, 75.
Woosley, S. E.: 1987, *Astrophys. J.* (in press).
Woosley, S. E., Pinto, P., and Ensman, L.: 1987a, *Astrophys. J.* **324**.
Woosley, S. E., Pinto, P. A., Martin, P. G., and Weaver, T. A.: 1987b, *Astrophys. J.* **318**, 664.
Wilson, J. R., Mayle, R., Woosley, S. E., and Weaver, T.: 1986, *Ann. N.Y. Acad. Sci.* **470**, 267.
Xu, Y., Sutherland, P., McCray, R., and Ross, R. R.: 1987, *Astrophys. J.* **327**.